Mössbauer Diffraction. II. Dynamical Theory of Mössbauer Optics*

J. P. HANNON
Physics Department, Rice University, Houston, Texas 77001

AND

G. T. TRAMMELL†
Physik-Department der Technischen Hochschule München, München, Germany

(Received 26 February 1969)

The dynamical theory of Mössbauer optics is developed utilizing the multiple-scattering equations derived in the preceding paper (I). The general optical equations obtained are analogous to the equations of the dynamical theory of x-ray diffraction, but are generalized to account for the very strong polarization mixing which occurs in Mössbauer optics. This polarization mixing leads to a number of interesting features, such as Faraday effects, selective absorption, and selective critical reflection. The cases of Bragg reflection, Laue transmission, critical reflection, and off-Bragg transmission are treated in detail.

I. INTRODUCTION

IN a preceding paper[1] we used the Feynman techniques of quantum electrodynamics to obtain the equations governing the interaction of γ rays and x rays with a system of scatterers.

The purpose of this paper is to utilize these multiple-scattering equations to develop the dynamical theory of Mössbauer optics.

Much of the theory, of course, is directly parallel to the dynamical theory of x-ray diffraction,[2–5] but it is necessary to generalize the x-ray theory to account for the very strong polarization mixing which occurs in Mössbauer optics. This polarization mixing leads to a number of interesting features, such as Faraday effects, selective absorption, and selective critical reflection.

Some features of the dynamical theory have been considered in Refs. 6–17, but these aspects have excluded the polarization mixing effects (with the exception of Refs. 14 and 15). The present paper is the first general treatment of the dynamical theory of Mössbauer optics.

In Sec. II, we first discuss the general form of the scattering operators, in Sec. III the dynamical theory is developed using a Darwin-Prins-type approach. The Laue formulation of Mössbauer optics is given in Appendix D.

In Sec. III A we treat the cases of Bragg reflection and Laue transmission. As discussed in a preceding paper,[6] and developed in more detail here, when a crystal containing resonant nuclei is excited at a Bragg angle, there is an enhancement of the effective coherent elastic radiative width and a consequent suppression of absorptive and inelastic processes which leads to large reflection and/or transmission amplitudes.

In Sec. III B we treat the off-Bragg transmission through a Mössbauer medium. We show for this case that there are two generally nonorthogonal eigenwaves in a Mössbauer medium which have different complex indices of refraction. The general expressions are given for the polarization and amplitude of the transmitted wave, and we discuss the associated Faraday effects.

In Sec. III C we treat the case of grazing incidence, and discuss the selective critical reflection of the eigenwaves.

II. SCATTERING FROM A MÖSSBAUER ATOM

In I, the multiple-scattering equations were developed in terms of the scattering operators $M_{\mu\nu}{}^{(j)}$ of the individual scatterers. For an arbitrary incident field $A_\nu{}^{(j)}$, $M_{\mu\nu}{}^{(j)}$ determines the scattering "response" of the jth

* Work supported in part by the Office of Naval Research under project THEMIS.

† On leave from Rice University.

[1] J. P. Hannon and G. T. Trammell, Phys. Rev. **169**, 315 (1968), hereafter referred to as I.

[2] M. von Laue, *Röntgenstrahleninterferenzen* (Becker and Erler, Liepzig, 1941), Chap. V.

[3] R. W. James, *The Optical Principles of Diffraction of X-Rays* (G. Bell and Sons, Ltd., London, 1948), pp. 52–92, 413–438, and 632–653.

[4] W. H. Zachariasen, *Theory of X-Ray Diffraction in Crystals* (John Wiley & Sons, Inc., New York, 1954), Chap. III.

[5] A quantum theory of x-ray diffraction is given by Martin Ashkin and Masao Kuryama, Proc. Phys. Soc. Japan **21**, 1549 (1966). We note that although these authors were concerned exclusively with x-ray diffraction, their theory can be applied to Mössbauer optics when the generalized polarizability Γ_{ij} is modified to take into account the sharp resonant Mössbauer scattering.

[6] G. T. Trammell, *Chemical Effects of Nuclear Transformations* (International Atomic Energy Agency, Vienna, 1961), Vol. I, p. 75.

[7] C. Muzikar, Zh. Eksperim. i Teor. Fiz. **41**, 1168 (1961) [English transl.: Soviet Phys.—JETP **14**, 833 (1962)].

[8] M. I. Podgoretskii and I. I. Raizen, Zh. Eksperim. i Teor. Fiz. **39**, 1473 (1960) [English transl.: Soviet Phys.—JETP **12**, 1023 (1961)].

[9] G. T. Trammell, Phys. Rev. **126**, 1045 (1962).

[10] S. Bernstein and E. C. Campbell, Phys. Rev. **132** 1625 (1963).

[11] A. M. Afanas'ev and Yu. Kagan, Zh. Eksperim. i Teor. Fiz. **48**, 327 (1965) [English transl.: Soviet Phys.—JETP **21**, 215 (1965)].

[12] J. P. Hannon and G. T. Trammell, Bull. Am. Phys. Soc. **10**, 162 (1965); **11**, 771 (1966).

[13] M. K. F. Wong, Proc. Phys. Soc. (London) **85**, 723 (1965).

[14] J. P. Hannon, M. A. thesis, Rice University, 1965 (unpublished); Ph.D. thesis, Rice University, 1967 (unpublished).

[15] M. Blume and O. C. Kistner, Phys. Rev. **171**, 417 (1968).

[16] D. A. O'Connor, Proc. Roy. Soc. (London) **1**, 973 (1968).

[17] Yu. M. Kagan, A. M. Afanas'ev, and I. P. Perstnev, Zh. Eksperim. i Teor. Fiz. **54**, 1530 (1968) [English transl.: Soviet Phys.—JETP **27**, 819 (1968)].

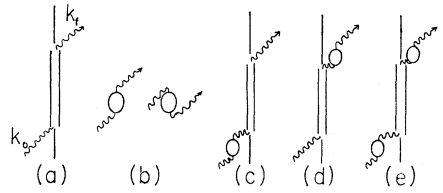

FIG. 1. Feynman diagrams representing the scattering processes from a Mössbauer atom.

atom, i.e., the coupling to the incident wave, and the amplitude and polarization of the scattered photon. For Mössbauer scattering this response is quite complex, depending upon the direction of incidence, the polarization and frequency of the incident photon, the structure and time dependence of the internal fields at the nucleus, and the direction of the scattered photon. In this section we give a brief discussion of the explicit form of $M_{\mu\nu}$ for a Mössbauer atom.

In terms of the nuclear and electronic Heisenberg current operators $J_\mu(x)$ and $j_\mu(x)$, the scattering operator is given by [Eq. (2) of I]

$$\begin{aligned} M_{\mu\nu}{}^{f0}(x,y) &= -(i/\hbar c^2)\langle\phi_f|T([J_\mu(x)+j_\mu(x)] \\ &\quad\times[J_\nu(y)+j_\nu(y)])|\phi_0\rangle \\ &= -(i/\hbar c^2)\langle\phi_f|T(J_\mu(x)J_\nu(y)+j_\mu(x)j_\nu(y) \\ &\quad+J_\mu(x)j_\nu(y)+j_\mu(x)J_\nu(y))|\phi_0\rangle, \quad (1) \end{aligned}$$

where ϕ_0 and ϕ_f are the initial and final Heisenberg state vectors of the crystal and T is the time-ordering operator.

The first two terms, $T(J_\mu(x)J_\nu(y))$ and $T(j_\mu(x)j_\nu(y))$, give the nuclear and electronic scattering operators, corresponding to Figs. 1(a) and 1(b). The remaining two terms, $T(J_\mu(x)j_\nu(y))$ and $T(j_\mu(x)J_\nu(y))$, give the "screening" processes, corresponding to Figs. 1(c) and 1(d). The second-order screening process, represented by Fig. 1(e), is obtained from $T(j_\mu(x)j_\nu(y))$. In the notation of I, the processes in Figs. 1(a) and 1(c)–1(e) contribute to the resonant scattering operator $N_{\mu\nu}$, while 1(b) gives the nonresonant electronic scattering operator $E_{\mu\nu}$.

A. Sharp Resonant Scattering

We first consider the contribution of $T(J_\mu(x)J_\nu(y))$ to the sharp resonant scattering by the nucleus [Fig. 1(a)]. As discussed in Appendix A, this leads to the contribution to the Feynman potential of the scattered photon:

$$\begin{aligned} &[A_\mu{}^s(\mathbf{z})]^{f0} \\ &=\delta_{z,i}{}^+(k_f)[N_{\mu\nu}{}^{(i)}(\mathbf{k}_f,\mathbf{k}_0)]^{f0}A_\nu{}^0(\mathbf{R}_i), \\ &=\delta_{z,i}{}^+(k_f)\langle\chi_f|e^{-i\mathbf{k}_f\cdot\mathbf{r}_i}|\chi_0\rangle \\ &\quad\times\sum_n[J_\mu{}^{fn}(-\mathbf{k}_f)J_\nu{}^{n0}(\mathbf{k}_0)(k_0-E_n+E_0+\tfrac{1}{2}i\Gamma_n)^{-1}] \\ &\quad\times\langle\chi_0|e^{i\mathbf{k}_0\cdot\mathbf{r}_i}|\chi_0\rangle A_\nu{}^0(\mathbf{R}_i). \quad (2) \end{aligned}$$

In Eq. (2), $\mathbf{k}_0$, is the wave vector of the incident photon, and

$$\mathbf{k}_f=[k_0-(E_f+\epsilon_f-E_0-\epsilon_0)]\frac{(\mathbf{z}-\mathbf{R}_i)}{|\mathbf{z}-\mathbf{R}_i|}$$

is the wave vector of the scattered photon; $\delta_{z,i}{}^+(k_f)=|\mathbf{z}-\mathbf{R}_i|^{-1}e^{ik_f|\mathbf{z}-\mathbf{R}_i|-i\omega_f t_z}$, and $A_\mu{}^0(\mathbf{x})e^{-i\omega_0 t_z}$ is the Feynman potential of the incident photon. In the first line of Eq. (2), the superscripts 0, f refer to the initial and final states $|\phi_0,\chi_0\rangle$, $|\phi_f,\chi_f\rangle$. Here ϕ represents the state of the crystal, excluding the vibrational state, and E represents its energy (e.g., ϕ includes the magnetic state of the crystal and the internal state of the nucleus), while χ and ϵ represent the vibrational state and vibrational energy, respectively. In the second line of Eq. (2),

$$J_\mu(\pm\mathbf{k})=\int e^{\pm i\mathbf{k}\cdot\mathbf{x}}J_\mu(\mathbf{x})d\mathbf{x}$$

is the Fourier transform of the current density $J_\mu(\mathbf{x})$, and the superscripts fn ($n0$) indicate the matrix element of $J_\mu(\pm\mathbf{k})$ between the states ϕ_f and ϕ_n (ϕ_n and ϕ_0). Finally, Γ_n is the total width of the excited state ϕ_n, including the radiation width Γ_γ, and the internal conversion width Γ_α.

In the fast relaxation cases (relaxation times very much smaller than the nuclear Larmor precession times τ_L), we may take ϕ and E in Eq. (2) as the state and energy of the nucleus i in the external fields and the "static effective fields" of the surrounding medium. Similarly, in the slow relaxation limit, ϕ and E may be taken as the state and energy of the *atom* i, but unless the hyperfine energy is negligible relative to the electronic Larmor frequency, one can no longer consider the transitions between nuclear states in an effective field but must allow for the dynamic effects of the nucleus on the atomic electrons, and treat the nucleus plus atomic electrons as a coupled quantum-mechanical system.[18] The modifications necessary when the relaxation times are on the order of τ_L are discussed briefly in Appendix A.

In terms of the scattering operator $(N_{\mu\nu}{}^{(i)})^{f0}$ of Eq. (2), the amplitude for scattering an incident photon with wave vector $\mathbf{k}_0$ and polarization $\boldsymbol{\epsilon}_0$ into a photon with wave vector $\mathbf{k}_f$ and polarization $\boldsymbol{\epsilon}_f$, with a change of the crystalline vibration state from χ_0 to χ_f, and change of the internal atomic state from ϕ_0 to ϕ_f, is given by

$$(f(\mathbf{k}_f,\boldsymbol{\epsilon}_f;\mathbf{k}_0,\boldsymbol{\epsilon}_0))^{f0}=\epsilon_\mu{}^{f*}(N_{\mu\nu}{}^{(i)}(\mathbf{k}_f,\mathbf{k}_0))^{f0}\epsilon_\nu{}^0. \quad (3)$$

Multipole expansion. The Mössbauer transitions are generally good multipole transitions [e.g., $M(1)$, $E(2)$, etc.], or a multipole mixture [e.g., $M(1)$-$E(2)$, etc.]. For simplicity, we consider the fast relaxation case,

[18] L. P. Hirst considers this problem in relation to his results on Mössbauer absorption measurements in dilute rare-earth alloys (unpublished).

where the effective fields acting on the nucleus have a common axis of symmetry ($\hat{z}$), so that the ground and excited nuclear states are states of good J_z. The generalizations when J_z is not conserved are given in Appendix C.

Making a multipole expansion of the four vectors $J(\mathbf{x})e^{\pm i\mathbf{k}\cdot\mathbf{x}}$ in terms of the vector spherical harmonics $\mathbf{Y}_{LM}^{(\lambda)}(\mathbf{k})$, and evaluating the reduced nuclear matrix elements in terms of the multipole radiative widths $\Gamma_\gamma(L,\lambda)$, the scattering amplitude is given by (see Appendix B and Refs. 9, 15, and 19–21)

$$(f(\mathbf{k}_f,\boldsymbol{\varepsilon}_f;\mathbf{k}_0,\boldsymbol{\varepsilon}_0))^{f0}=(4\pi/k_0)\langle\chi_f|e^{-i\mathbf{k}_f\cdot\mathbf{r}_i}|\chi_0\rangle\langle\chi_0|e^{i\mathbf{k}_0\cdot\mathbf{r}_i}|\chi_0\rangle \times\sum_{L'\lambda'}\sum_{L\lambda}C(j_0L'j_n;m_0'M'm_n)C(j_0Lj_n;m_0Mm_n)\boldsymbol{\varepsilon}_f^*\cdot\mathbf{Y}_{L'M'}^{(\lambda')}(\mathbf{k}_f)\mathbf{Y}_{LM}^{(\lambda)}(\mathbf{k}_0)^*\cdot\boldsymbol{\varepsilon}_0[\Gamma_\gamma(L',\lambda')\Gamma_\gamma(L,\lambda)]^{1/2} \times\Gamma^{-1}[\exp i(\eta_{L'}{}^{\lambda'}-\eta_L{}^{\lambda})][x(m_0M)-i]^{-1}, \quad (4)$$

where $x(m_0M)=2[E(j_n,\,m_0+M)-E(j_0,m_0)-k_0]/\Gamma$, $M=m_n-m_0$, $M'=M=m_0-m_0'$, the notation for the Clebsch-Gordan coefficients is that of Rose,[22] and (L,λ), $\lambda=0$ or 1 designates the multipole $[(L,1)\equiv E(L)=$electric 2^L pole, $(L,0)\equiv M(L)=$magnetic 2^L pole$]$. The $i\eta_L{}^{\lambda}$, as defined by Eq. (B8), give the phase of the reduced nuclear matrix elements (for emission). If T invariance is valid, then $\eta_{L'}{}^{\lambda'}-\eta_L{}^{\lambda}=0$ or π.[23]

For some purposes it is convenient to have the scattering amplitude expressions in terms of the right- and left-hand circularly polarized bases $\boldsymbol{\eta}^{(\pm)}=\mp(\mathbf{e}_\theta\pm i\mathbf{e}_\phi)/\sqrt{2}$. From Eq. (B7), we obtain

$$\boldsymbol{\eta}_{\mu'}{}^*\cdot\mathbf{Y}_{L'M'}^{(\lambda')}(\mathbf{k}_f)\,\mathbf{Y}_{LM}^{(\lambda)}(\mathbf{k}_0)^*\cdot\boldsymbol{\eta}_\mu =(8\pi)^{-1}(\mu')^{\lambda'+1}(\mu)^{\lambda+1}[(2L'+1)(2L+1)]^{1/2} \times\mathfrak{D}_{\mu'M'}^{(L')}(\hat{k}_f,\hat{z})\mathfrak{D}_{\mu M}^{(L)}(\hat{k}_0,\hat{z})^*, \quad (5)$$

where the notation for the rotation matrices $\mathfrak{D}$ is that of Rose,[22] and $\mu,\ \mu'=\pm1$. The scattering amplitude $(f(\mathbf{k}_f,\boldsymbol{\eta}_{\mu'};\mathbf{k},\boldsymbol{\eta}_\mu))^{f0}$ is then given by (4) with the substitution (5).

B. Electronic Scattering

The electronic scattering processes are well known and careful treatments can be found in Refs. 2–4. Here we give only a brief outline of the electronic scattering from a Mössbauer atom.

Equation (A12) gives the scattering operator to order e^2 if we take $j_\mu(\mathbf{x})=e{:}\bar{\psi}(\mathbf{x})\gamma_\mu\psi(\mathbf{x}){:}$, where we mean by : : the Wick normal product and include the filled negative-energy sea as well as the normally occupied positive-energy electron states in $v(\mathbf{x})$.[24] It will be sufficient for our purposes to treat the electrons in the nonrelativistic approximation. In the sum over the negative-energy k's of (A12) the energy denominators may be replaced by $-2mc^2$, and after some manipulation[25] this term results in the nonrelativistic A^2 scattering term, which from the relativistic point of view is due to the presence of the atomic electrons inhibiting virtual pair production. In the remaining sum over positive energy k's and p's, we may take the Pauli nonrelativistic form for the current operators $j_\mu(x)$.[26] We then obtain the expression

$$E_{\mu\nu}(x,y)=(e/m)\delta_{\mu\nu}(1-\delta_{4\mu})\delta(x-y)\rho(\mathbf{x})+T(j_\mu(x)j_\nu(y)), \quad (6)$$

where

$$\rho(\mathbf{x})=j_4(\mathbf{x})=e\sum_i\delta(\mathbf{x}-\mathbf{x}_i), \quad (7)$$

$$\mathbf{j}(\mathbf{x})=(e/2m)\sum_i[\mathbf{p}_i\delta(\mathbf{x}-\mathbf{x}_i)+\delta(\mathbf{x}-\mathbf{x}_i)\mathbf{p}_i +i\delta(\mathbf{x}-\mathbf{x}_i)\mathbf{p}_i\times\boldsymbol{\sigma}_i-i\mathbf{p}_i\times\boldsymbol{\sigma}_i\delta(\mathbf{x}-\mathbf{x}_i)]. \quad (8)$$

In (6)–(8) e is the electron charge, the summation is over the atomic electrons, and the operators referring to the electrons are the usual nonrelativistic Heisenberg operators for the atomic electrons. The Rayleigh electronic scattering is given by the first term in (6), while the photoelectric dispersion and anomolous scattering are given by the second term.

It is easily verified that the nonrelativistic form for $E_{\mu\nu}(x,y)$ satisfies $\partial_{x^\mu}E_{\mu\nu}(x,y)=\partial_{y^\nu}E_{\mu\nu}(x,y)=0$, so that gauge invariance is manifest.

For many cases the Mössbauer frequency is large in comparison with any natural electronic absorption frequency, and the scattering amplitude obtained from (6) is then [to order $(v/c)^2$]

$$(f_e(\mathbf{k}_f,\boldsymbol{\varepsilon}_f;\mathbf{k}_0,\boldsymbol{\varepsilon}_0))^{f0}=\boldsymbol{\varepsilon}_f{}^*\cdot\boldsymbol{\varepsilon}_0\langle\chi_f|e^{-i(\mathbf{k}_f-\mathbf{k}_0)\cdot\mathbf{r}_i}|\chi_0\rangle \times[-(e^2/mc^2)F(\theta)+i(k_0/4\pi)\sigma_{pe}], \quad (9)$$

where $F(\theta)=\langle e_0|\sum_i e^{i(\mathbf{k}_0-\mathbf{k}_f)\cdot\mathbf{x}_i}|e_0\rangle$ is the electronic form factor, and σ_{pe} is the photoelectric cross section. In this approximation the polarization response is that of an isotropic electric dipole oscillator, and gives no polarization mixing. The inclusion of more complicated electronic scattering processes, such as small polarization mixing terms on anomolous scattering, does not alter the general optical theory presented in Sec. III.

C. Screening Effects

As discussed in a preceding paper,[20] when the "screening" processes represented by Figs. 1(c)–1(e) are added to the direct nuclear scattering process of Fig.

[19] H. Frauenfelder, D. E. Nagle, R. D. Taylor, D. R. F. Cochran, and W. M. Visscher, Phys. Rev. **126**, 1065 (1962).
[20] J. P. Hannon and G. T. Trammell, Phys. Rev. Letters **21**, 726 (1968).
[21] R. W. Hayward, in *Handbook of Physics*, edited by E. V. Condon and Hugh Odishaw (McGraw-Hill Book Co., New York, 1967), Part 9, Chap. 6, p. 172.
[22] M. E. Rose, *Elemenatry Theory of Angular Momentum* (John Wiley & Sons, Inc., New York, 1957), pp. 32–48.
[23] S. P. Lloyd, Phys. Rev. **83**, 716 (1951).
[24] G. C. Wick, Phys. Rev. **80**, 268 (1950).
[25] See for example, R. P. Feynman, *Quantum Electrodynamics* (W. A. Benjamin, Inc., New York, 1958), p. 153.
[26] A. Messiah, *Quantum Mechanics* (North-Holland Publishing Co., Amsterdam, 1965), Vol. II, p. 937.

1(a), the effect is to replace $\mathbf{e}_f^*\cdot\mathbf{J}^{fn}(-\mathbf{k}_f)$ in Eq. (2) by $\mathbf{e}_f^*\cdot\mathfrak{J}^{fn}(-\mathbf{k}_f)$, which in a multipole expansion is given by

$$\mathbf{e}_f^*\cdot\mathfrak{J}^{fn}(-\mathbf{k}_f)=\sum_{\lambda LM}\mathbf{e}_f^*\cdot\mathbf{Y}_{LM}^{(\lambda)}(\mathbf{k}_f)(1+E_L^\lambda)\times\langle f|\int\mathbf{A}_{LM}^{(\lambda)}(\mathbf{x})\cdot\mathbf{J}(\mathbf{x})d\mathbf{x}|n\rangle,\quad(10)$$

where λ is only to be summed over 1 and 0 in (10). E_L^λ represents the effect of the atomic electrons on the outgoing wave from the nucleus, and is given by

$$E_L^\lambda=\frac{ik}{4\pi}\int d\mathbf{x}d\mathbf{y}\sum_p[\langle 0|\mathbf{j}(\mathbf{x})\cdot\mathbf{A}_{LM}^{(\lambda)}(\mathbf{x})^*|p\rangle\times\langle p|B_{LM}^\lambda(\mathbf{y})|0\rangle(E_0+k+i\epsilon-E_p)^{-1}+\langle 0|B_{LM}^\lambda(\mathbf{y})|p\rangle\langle p|\mathbf{j}(\mathbf{x})\cdot\mathbf{A}_{LM}^{(\lambda)}(\mathbf{x})^*|0\rangle\times(E_0+i\epsilon-k-E_p)^{-1}],\quad(11)$$

where

$$B_{LM}^{(0)}(\mathbf{y})=-\mathbf{j}(\mathbf{y})\cdot\mathbf{B}_{LM}^{(0)}(k\mathbf{y}),$$
$$B_{LM}^{(1)}(\mathbf{y})=-\mathbf{j}(\mathbf{y})\cdot\mathbf{B}_{LM}^{(1)}(k\mathbf{y})+(L/L+1)^{1/2}\times[\rho(\mathbf{y})\Phi_{LM}(k\mathbf{y})-\mathbf{j}(\mathbf{y})\cdot\mathbf{B}_{LM}^{(-1)}(k\mathbf{y})].\quad(12)$$

The vector spherical notation in Eqs. (10)–(12) is that of Akhiezer and Berestetskii[27] (also see Rose[28]), and the basic definitions are summarized in Appendix B.

In (10) and (11) we have assumed that the effect of the unfilled electronic shells is negligible, so that E_L^λ does not depend upon M or the direction of $\mathbf{k}_f$.

Similarly, $\mathbf{J}^{n0}(\mathbf{k}_0)\cdot\mathbf{e}_0$ in Eq. (2) is replaced by $\mathfrak{J}^{n0}(\mathbf{k}_0)\cdot\mathbf{e}_0$,

$$\mathfrak{J}^{n0}(\mathbf{k}_0)\cdot\mathbf{e}_0=\sum_{\lambda LM}\langle n|\int d\mathbf{x}\,\mathbf{A}_{LM}^{(\lambda)}(\mathbf{x})\cdot\mathbf{J}(\mathbf{x})|0\rangle\times(1+E_L^\lambda)\mathbf{Y}_{LM}^{(\lambda)}(\mathbf{k}_0)^*\cdot\mathbf{e}_0,\quad(13)$$

where E_L^λ is again given by (11).

The real part of E_L^λ gives the effect of the induced electronic currents in (or 180° out of) phase with the nuclear currents, and gives a small correction to the nuclear radiation width which we may neglect. The imaginary part of E_L^λ, although quite small ($\approx 10^{-3}$–10^{-1} rad), is of importance in analyzing the results of T-invariance experiments,[20,29] and in certain cases, such as for the 6.25-keV Ta^{181} $E1$ γ ray, gives an observable dispersion effect in the absorption spectrum.[30,31]

Writing $E_L^\lambda=i\xi_L^\lambda$, we see that the effects of the screening processes are given by making the replacement

$$\exp i(\eta_{L'}^{\lambda'}-\eta_L^\lambda)\rightarrow(1+i\xi_{L'}^{\lambda'})[\exp i(\eta_{L'}^{\lambda'}-\eta_L^\lambda)](1+i\xi_L^\lambda)\simeq\exp i(\eta_{L'}^{\lambda'}-\eta_L^\lambda+\xi_{L'}^{\lambda'}+\xi_L^\lambda)\quad(14)$$

in Eq. (4).

(*i*) *Conversion screening.* The principal contribution to the imaginary part of E_L^λ comes from the conversion pole term in (11),

$$i\xi_L^\lambda\doteq\tfrac{1}{4}k\sum_p\delta(E_0+k-E_p)\langle 0|\int d\mathbf{x}\,\mathbf{j}(\mathbf{x})\cdot\mathbf{A}_{LM}^{(\lambda)}(\mathbf{x})|p\rangle\times\langle p|\int d\mathbf{y}\,B_{LM}^{(\lambda)}(\mathbf{y})|0\rangle.\quad(15)$$

The $B_{LM}^{(\lambda)}$ matrix element appearing in (15) is that which is involved in internal-conversion coefficient calculations, while the $A_{LM}^{(\lambda)}$ matrix element is that involved in (L,λ) photoelectron emission.

Using the relativistic form for the electronic current density, $\mathbf{j}(\mathbf{x})=\sum_i\boldsymbol{\alpha}^{(i)}\delta(\mathbf{x}-\mathbf{x}_i)$, and following Rose's development for calculating the internal-conversion coefficient,[28,32] we obtain the following expressions for the ML and EL conversion screening:

$$i\xi(ML)\equiv i\xi_L^0=-\pi\alpha k[L(L+1)(2L+1)]^{-1}\times\sum_{\mu\mu'}B_{\mu\mu'}r_{\mu\mu'}(m)R_{\mu\mu'}(m),\quad(16)$$

$$i\xi(EL)\equiv i\xi_L^1=-\pi\alpha k[L(L+1)(2L+1)]^{-1}\times\sum_{\mu\mu'}C_{\mu\mu'}r_{\mu\mu'}(e)R_{\mu\mu'}(e).\quad(17)$$

The notation used in Eqs. (16) and (17) is that of Rose: $k=\hbar\omega_0/mc^2$, $\alpha=1/137$, and

$$R_{\mu\mu'}(m)=\int_0^\infty h_L^{(1)}(kr)[f_\mu(pr)g_{\mu'}+g_\mu(pr)f_{\mu'}]r^2dr,\quad(18)$$

$$R_{\mu\mu'}(e)=(\mu-\mu')\int_0^\infty h_{L-1}^{(1)}(kr)\times[f_\mu(pr)g_{\mu'}+g_\mu(pr)f_{\mu'}]r^2dr+L\int_0^\infty\{h_{L-1}^{(1)}(kr)[f_\mu(pr)g_{\mu'}-g_\mu(pr)f_{\mu'}]-h_L^{(1)}[f_\mu(pr)f_{\mu'}+g_\mu(pr)f_\mu]\}r^2dr.\quad(19)$$

[27] A. I. Akhiezer and V. B. Berestetskii, *Quantum Electrodynamics* (Wiley-Interscience Publishers, Inc., New York, 1965), pp. 27–29, 537–541.

[28] M. E. Rose, in *Alpha-, Beta-, and Gamma-Ray Spectroscopy*, edited by K. Sieghan (North-Holland Publishing Co., Amsterdam, 1965), Vol. II, Chap. XVI, p. 887.

[29] A detailed analysis of such experiments using the dynamical theory developed in this paper is presently being written up for publication.

[30] C. Sauer, E. Matthias, and R. L. Mössbauer, Phys. Rev. Letters **21**, 961 (1968).

[31] G. T. Trammell and J. P. Hannon, Phys. Rev. **180**, 337 (1969).

[32] M. E. Rose, *Internal Conversion Coefficients* (North-Holland Publishing Co., Amsterdam, 1958).

The $r(m)$ and $r(e)$ integrals appearing in (16) and (17) are given by[33]

$$r_{\mu\mu'}(m)=\int_0^\infty j_L(kr)[f_\mu(pr)g_{\mu'}+g_\mu(pr)f_{\mu'}]r^2dr, \quad (20)$$

$$r_{\mu\mu'}(e)=\tfrac{1}{2}(L-\mu'+\mu)\int_0^\infty j_{L-1}(kr)f_\mu(pr)g_{\mu'}r^2dr$$
$$-\tfrac{1}{2}(L+\mu'-\mu)\int_0^\infty j_{L-1}(kr)g_\mu(pr)f_{\mu'}r^2dr$$
$$+\left(\frac{L}{2L+2}\right)(L+1+\mu'-\mu)\int_0^\infty j_{L+1}(kr)$$
$$\times f_\mu(pr)g_{\mu'}r^2dr-\left(\frac{L}{2L+2}\right)(L+1-\mu'+\mu)$$
$$\times\int_0^\infty j_{L+1}(kr)g_\mu(pr)f_{\mu'}r^2dr. \quad (21)$$

In (18)–(21), $g_{\mu'}$ and $f_{\mu'}$ are the upper and lower component radial wave functions for the bound state, and $g_\mu(pr)$ and $f_\mu(pr)$ are the radial wave functions for the continuum state. In (18) and (19) the $h_L^{(1)}$'s are spherical Hankel functions of the first type, and in (21) and (22) the j_L's are spherical Bessel functions. Finally, the coefficients $B_{\mu\mu'}$ and $C_{\mu\mu'}=B_{-\mu\mu'}/(\mu-\mu')^2$ are given in Table (b) of Ref. 33.

The dominant contributions to (16) and (17) come from the inner electronic shells for which $kr\ll 1$. In this region $h_L(kr)\sim -i(kr)^{-L-1}$, while $j_L(kr)\sim(kr)^L$.

We have computed the $\xi_L{}^\lambda$ for the 90-keV Ru^{99} and the 73-keV Ir^{193} Mössbauer transition, and obtained

$$\xi_{Ru}(E2)=-6.7\times10^{-3},\quad \xi_{Ru}(M1)=-0.2\times10^{-3},$$
$$\xi_{Ir}(E2)=+1.4\times10^{-3},\quad \xi_{Ir}(M1)=+0.5\times10^{-3}. \quad (22)$$

In making these computations, we used the tabulated values of the $R_{\mu\mu'}$ given by Rose[32] and by Band, Listengarten, and Sliv.[34] The $r_{\mu\mu'}$ integrals were computed using Dirac Coulomb wave functions. We also mention that the K-shell conversion channel is closed for the 73-keV Ir^{193} transition, and the Ir results in (22) represent the L-shell contribution,

We note that the sign of the $\xi_L{}^\lambda$ can be either (+) or (−), and there is some destructive interference among the various contributions of (16) and (17). Unless there is strong cancellation, however, we will usually have $|\xi(E2)|>|\xi(M1)|$. This occurs because of the suppression of the $r_{\mu\mu'}(M1)$ matrix element. This latter point is most easily seen from the nonrelativistic approximation of the $\langle 0|\mathbf{j}\cdot\mathbf{A}_{1M}{}^0|p\rangle$ matrix element, which gives the leading term proportional to $\langle 0\|\mathbf{M}\|p\rangle$, where $\mathbf{M}$ is the magnetic moment operator. In the derivation of (16) and (17) a Russell-Saunders–type approximation is used for the electronic wave functions. For this case, however, as discussed by Bethe and Salpeter,[35] $\langle 0\|\mathbf{M}\|p\rangle=0$ unless the states belong to the same fine structure multiplet.

(*ii*) *Rayleigh screening.* Away from the absorption edge, the primary real contribution to $E_L{}^\lambda$ comes from the Rayleigh term of $E_{\mu\nu}$. Making the nonrelativistic approximation as in Eq. (6), and taking the electronic ground-state wave function $|e_0\rangle$ as a product of wave functions of the form

$$R_{nl}(x)Y_{lm}(\mathbf{x})\begin{pmatrix}\alpha\\ \beta\end{pmatrix},$$

then for a mixed $M(L)-E(L+1)$ transition the Rayleigh screening contribution gives

$$R_L\equiv E_{L+1}{}^1=E_L{}^0=-izk_0r_0\langle j_L(k_0r)h_L{}^{(1)}(k_0r)\rangle. \quad (23)$$

In Eq. (23) $r_0=e^2/mc^2$ and

$$\langle j_Lh_L{}^{(1)}\rangle=\sum_{n,l}(4l+2)\langle R_{nl}|\,j_Lh_L{}^{(1)}\,|R_{nl}\rangle/Z.$$

We see from (23) that the Rayleigh screening gives identical shifts to photons emitted by $M(L)$ and $E(L+1)$ nuclear transitions. To obtain an upper estimate of R_L, we assume $k_0r\ll 1$ for all electronic shells. Then

$$j_Lh_L{}^{(1)}\approx -i[(2L+1)k_0r]^{-1}$$

and

$$R_L\approx -zr_0(2L+1)^{-1}\langle 1/r\rangle.$$

Taking $\langle 1/r\rangle\approx z^{1/3}/a_0$, then

$$R_L\approx -z^{4/3}[(2L+1)(137)^2]^{-1},$$

which gives $R_1\approx -2.8\times10^{-3}$ for Ru^{99} and $R_1\approx -5.8\times10^{-3}$ for Ir^{193}. We can generally neglect R_L, since it is primarily real and much less than unity.

III. DYNAMICAL THEORY OF MÖSSBAUER OPTICS

The multiple-scattering equations which describe the interaction of a γ ray with a Mössbauer medium are given by Eqs. (50) and (51) of I. These equations are identical in form to the semiclassical equations used to develop the dynamical theory of x-ray diffraction,[2–5] and as a consequence, much of the x-ray theory can be taken over directly. However, it is necessary to generalize the x-ray theory to account for the very strong polarization mixing which occurs in Mössbauer optics.

[33] There are, of course, a number of alternative expressions for the $r_{\mu\mu'}(e)$ which are obtained by utilizing the gauge invariance. See, for example, Ref. 27, p. 349.

[34] I. M. Band, M. A. Listengarten, and L. A. Sliv, in *Alpha-, Beta-, and Gamma-Ray Spectroscopy*, edited by K. Siegbahn (North-Holland Publishing Co., Amsterdam, 1965), Vol. II, pp. 1673–1680.

[35] H. A. Bethe and E. E. Salpeter, *Quantum Mechanics of One- and Two-Electron Atoms* (Academic Press Inc., New York, 1957), p. 282.

We will generally limit our discussion here to perfect single crystals (except for the cases of critical reflection and transmission off Bragg, where the expressions are independent of crystal structure). The reflection and transmission coefficients depend somewhat upon the shape of the crystal, and, as in the usual x-ray development, we take the form shown in Fig. 2(a): We assume that some set of infinite crystalline planes is parallel to the surface, which we take as the xy plane, and that the crystal is of finite thickness t in the z direction, $t=Md$, where M is the number of "planes," and d is the interplanar distance. The thickness of the layers is rather arbitrary, but they must be sufficiently thin so that the Born approximation is good within the layer. We generally assume a unit cell thickness (chemical or magnetic, whichever is larger). For example, if there is a magnetic spiral axis $\hat{\theta}$, it is convenient to use the magnetic unit cell, which contains the full spiral, so that each unit cell in the crystal has the same internal field structure. The assumption that one set of crystalline planes is parallel to the surface is slightly restrictive, but the resulting optical solutions are essentially the same as for the Laue formulation, where no such assumption is made (see Appendix D).

If a photon $A_\nu^0(z)=a_\nu^0 \exp i(\mathbf{k}_0\cdot\mathbf{z}-\omega_0 t_z)$ is incident on a plane layer (at $z=0$), then in the Born approximation the coherent elastic photon amplitude at R is given by[36]

$$A_\mu(\mathbf{R})=A_\mu^0(\mathbf{R})+A_\mu^s(\mathbf{R})$$
$$=A_\mu^0(\mathbf{R})+\sum_s (i\lambda_0 n'/\sin\phi_{(s)})$$
$$\times[\exp i(g_{(s)}|z|+(\mathbf{k}_{xy}^0+\boldsymbol{\tau}_{(s)})\cdot\mathbf{R})]$$
$$\times M_{\mu\nu}(-i\overleftarrow{\nabla}_{\mathbf{R}},\mathbf{k}_0)a_\nu^0, \quad (24)$$

where

$$g_{(s)}=[k_0^2-(\mathbf{k}_{xy}^0+\boldsymbol{\tau}_{(s)})^2]^{1/2}, \quad (25a)$$

$$\sin\phi_{(s)}=g_{(s)}/k_0, \quad (25b)$$

and n' is the number of unit cells/cm^2. $M_{\mu\nu}$ is understood to be the coherent scattering operator of the *unit cell*

$$M_{\mu\nu}(\mathbf{k}',\mathbf{k})=\sum_\rho [M_{\mu\nu}^{(\rho)}(\mathbf{k}',\mathbf{k})]_c e^{-i(\mathbf{k}'-\mathbf{k})\cdot\rho}. \quad (26)$$

The $\boldsymbol{\tau}_{(s)}$ in Eqs. (24) and (25) are the *planar* reciprocal-lattice vectors for the unit cells, and the sum is over all $\boldsymbol{\tau}_{(s)}$ for which $g_{(s)}$ is real (the sum over the $\boldsymbol{\tau}_s$ for which g_s is imaginary gives an exponentially damped contribution on the order of $e^{-k_0|z|/k_0|z|}$. The scattered photon amplitude is thus a superposition of a *finite* number of plane-wave channels $(s\pm)$ having wave vectors $\mathbf{k}_{(s\pm)}=(\pm g_{(s)},\mathbf{k}_{xy}^0+\boldsymbol{\tau}_{(s)})$. These channels are symmetric about the scattering plane, i.e., for each forward scattered wave in the $\mathbf{k}_{(s+)}$ direction [the $(s+)$ channel], there is a reflected wave in the $\mathbf{k}_{(s-)}$ direction [the $(s-)$ channel] [see Fig. 2(b)].

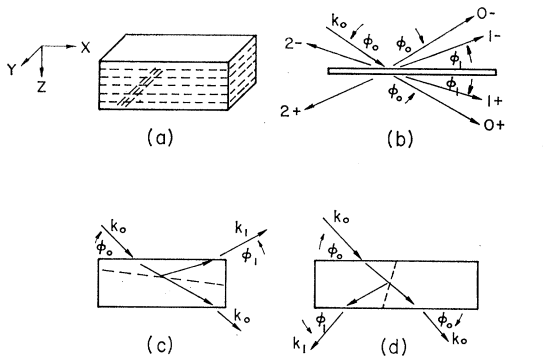

FIG. 2. (a) Schematic representation of the crystal geometry used in developing dynamical theory (dashed lines indicate crystal planes); (b) representation of open radiation channels for a plane layer; (c) Bragg reflection; (d) Laue transmission.

In a crystal of finite thickness, any wave of appreciable magnitude within the crystal is built up by constructive interference of the planar radiation channels. All the (open) planar channels contribute to the general dynamical equations [Eq. (27) below], but in the usual approximation, only constructively interfering channels need be considered open for the crystal. Thus, there will generally be only one or two radiation channels open in a crystal [off Bragg, only the $(0+)$ channel is open, for single-Bragg reflection, the $(0+)$ and a $(1-)$ channel are open, and for Laue transmission, the $(0+)$ channel and a $(1+)$ channel are open].

This approach to the problem follows the Darwin-Prins development of the dynamical x-ray diffraction. The alternative Laue formulation is discussed in Appendix D.[37]

The generalization of the Darwin-Prins dynamical equations is straightforward: Denoting by $A_\mu^{(m)}(\mathbf{k}_{(s+)})$ the wave incident on the mth plane (from "above") in the $(s+)$ channel, and similarly, by $A_\mu^{(m)}(\mathbf{k}_{(s-)})$ the wave incident on the mth plane (from "below") in the $(s-)$ channel, then the waves incident from above on the mth plane are related to the waves incident on the $(m-1)$th plane as given by

$$A_\mu^{(m)}(\mathbf{k}_{(s+1)})=e^{ig_{(s+)}d}[A_\mu^{(m-1)}(\mathbf{k}_{(s+)})+(i\lambda_0 nd/\sin\phi_{(s)})$$
$$\times\sum_{s'}\sum_{\eta=\pm} M_{\mu\nu}^{(m-1)}(\mathbf{k}_{(s+)},\mathbf{k}_{(s'\eta)})A_\nu^{(m-1)}(\mathbf{k}_{(s'\eta)})], \quad (27)$$

where d is the interplanar distance and n is the unit-cell density (cm^{-3}). $M_{\mu\nu}^{(m-1)}$ is the unit-cell scattering operator of the $(m-1)$th plane. We will generally limit our considerations to uniform Mössbauer crystals (i.e., crystals with a uniform distribution of Mössbauer

[36] An exact treatment of planar scattering, i.e., including mutliple scattering within the plane, is given in Refs. 6 and 15. The primary effect of the multiple scattering is to add a width contribution to the resonance denominator $\approx -\Gamma_\gamma\sigma$(coh. elastic scatt.)/$\sigma$(total), where Γ_γ is the radiative width for an isolated nucleus. For most cases this contribution is negligible.

[37] For a discussion of the Darwin-Prins and Laue formulations of the dynamical theory of x-ray diffraction, see, for example, Ref. 3, pp. 52–90, 413–436.

atoms, and for which the unit-cell internal field structure is the same throughout the crystal) for which the plane designation of the scattering operator can be omitted. Equation (27) is an obvious result: The amplitude that a wave $A_\mu(\mathbf{k}_{(s+)})$ is incident on the mth plane (from above) is equal to the amplitude that such a wave is incident on the $(m-1)$ plane, plus the forward scattering

$$i\frac{2\pi\lambda_0 nd}{\sin\phi_{(s)}}M_{\mu\nu}{}^{(m-1)}(\mathbf{k}_{(s+)},\mathbf{k}_{(s+)})A_\nu{}^{(m-1)}(\mathbf{k}_{(s+)})$$

of this wave by the $(m-1)$ plane, plus the amplitudes of all other channels incident on the $(m-1)$ plane being scattered into the $(s+)$ channel by this plane. These effects are propagated to the mth plane by the phase factor $e^{ig(s)d}$.

Similarly, the waves incident on the mth plane from below are related to the waves incident on the $(m+1)$ plane, with $A_\mu{}^{(m)}(\mathbf{k}_{(s-)})$ given by Eq. (27) with the replacements $(s+)\rightarrow(s-)$, $(m-1)\rightarrow(m+1)$.

Denoting the first plane as the $m=0$ plane, and the last plane as the $m=M$ plane, then the general boundary conditions to be satisfied are

$$A_\mu{}^{(m=0)}(\mathbf{k}_{(s+)})=\delta_{s0}a_\mu{}^0 e^{i\mathbf{k}_0\cdot\mathbf{R}_0}, \tag{28a}$$

$$A_\mu{}^{(m=M)}(\mathbf{k}_{(s-1)})=0. \tag{28b}$$

That is, the only wave incident from above on the first plane is $A_\mu{}^0$, and there are no waves incident from below on the last plane.

It has already been implicitly assumed in deriving Eq. (27) that $k_0 d\gg 1$, which is well satisfied for Mössbauer frequencies. Thus the longitudinal and scalar components need not be considered and it is convenient to express Eq. (27) in terms of orthogonal transverse amplitudes.

We define by $\boldsymbol{\varepsilon}_x{}^{(s\eta)}$, $\boldsymbol{\varepsilon}_y{}^{(s\eta)}(\eta=+\text{ or }-)$ any convenient orthogonal bases perpendicular to $\mathbf{k}_{(s\eta)}$. In terms of this basis, the transverse part of $A_\mu{}^{(m)}(\mathbf{k}_{(s\eta)})$ is given by

$$\mathbf{A}^{(m)}(\mathbf{k}_{(s+)})=(\boldsymbol{\varepsilon}_x{}^{(s+)}T_{x,m}{}^{(s)}+\boldsymbol{\varepsilon}_y{}^{(s+)}T_{y,m}{}^{(s+)})\times\exp i\mathbf{k}_{xy}{}^{(s+)}\cdot\mathbf{R}_m, \tag{29a}$$

$$\mathbf{A}^{(m)}(\mathbf{k}_{(s-1)})=(\boldsymbol{\varepsilon}_x{}^{(s-)}R_{x,m}{}^{(s)}+\boldsymbol{\varepsilon}_y{}^{(s-)}R_{y,m}{}^{(s)})\times\exp i\mathbf{k}_{xy}{}^{(s-)}\cdot\mathbf{R}_m, \tag{29b}$$

where

$$T_{x,m}{}^{(s)}=\boldsymbol{\varepsilon}_x{}^{(s+)*}\cdot\mathbf{A}^{(m)}(\mathbf{k}_{(s+)})\exp(-i\mathbf{k}_{(s+)}{}^{xy}\cdot\mathbf{R}_m),\text{ etc.},$$

so that $T_{x,m}{}^{(s)}$ gives the scalar amplitude that a photon $|\boldsymbol{\varepsilon}_x{}^{(s+)},\mathbf{k}_{(s+)}\rangle$ is incident on the mth layer from above, etc. We will denote the $(s+)$ channels by the index t, and the $(s-)$ channels by r, and define the column vectors $\mathbf{T}_m{}^t$, $\mathbf{R}_m{}^r$ as

$$\mathbf{T}_m{}^t=\begin{pmatrix}T_{x,m}{}^{(t)}\\ T_{y,m}{}^{(t)}\end{pmatrix}, \tag{30a}$$

$$\mathbf{R}_m{}^r=\begin{pmatrix}R_{x,m}{}^{(r)}\\ R_{y,m}{}^{(r)}\end{pmatrix}. \tag{30b}$$

The "planar" scattering matrix $\tilde{F}^{(ss')}$ (and $\tilde{f}^{(ss')}$) $(s,\ s'=t\text{ or }r)$ for scattering an (s') channel into an (s) channel is defined by

$$\tilde{F}^{(ss')}\equiv\frac{d}{\sin\phi_{(s)}}\tilde{f}^{(ss')}=\begin{pmatrix}F_{xx}{}^{ss'} & F_{xy}{}^{ss'}\\ F_{yx}{}^{ss'} & F_{yy}{}^{ss'}\end{pmatrix}, \tag{31}$$

where

$$F_{\lambda\lambda'}{}^{ss'}\equiv(d/\sin\phi_{(s)})f_{\lambda\lambda'}{}^{ss'}=(d/\sin\phi_{(s)})\lambda_0 n\boldsymbol{\varepsilon}_{\lambda\mu}{}^{(s)*}\times M_{\mu\nu}(\mathbf{k}_{(s)},\mathbf{k}_{(s')})\boldsymbol{\varepsilon}_{\lambda'\nu}{}^{(s')}, \tag{32}$$

$\lambda,\ \lambda'=x$ or y. The planar scattering amplitudes F are dimensionless, while the amplitudes f have the dimensions of a mass absorption coefficient, i.e., length^{-1}.

In terms of these matrix quantities, the dynamical equations for Mössbauer optics are given by the coupled equations

$$\mathbf{T}_m{}^t=e^{ig(t)d}(\mathbf{T}_{m-1}{}^t+i\sum_{t'}\tilde{F}^{(tt')}\mathbf{T}_{m-1}{}^{t'}+i\sum_r\tilde{F}^{(tr)}\mathbf{R}_{m-1}{}^r), \tag{33a}$$

$$\mathbf{R}_m{}^r=e^{ig(r)d}(\mathbf{R}_{m+1}{}^r+i\sum_{r'}\tilde{F}^{(rr')}\mathbf{R}_{m+1}{}^{r'}+i\sum_t\tilde{F}^{(rt)}\mathbf{T}_{m+1}{}^t), \tag{33b}$$

with the boundary conditions,

$$\tilde{\epsilon}^{(t)}\mathbf{T}_0{}^t=\delta_{t0}\mathbf{a}_0(\hat{k},\omega), \tag{34a}$$

$$\mathbf{R}_M{}^r=0. \tag{34b}$$

In (34), $\tilde{\epsilon}^{(t)}$ is the row vector $(\boldsymbol{\varepsilon}_x{}^t,\ \boldsymbol{\varepsilon}_y{}^t)$.

Equations (33) are the generalization of the Darwin-Prins equations of x-ray optics. These equations include not only the polarization mixing effects, but by including the contribution of all (open) planar radiation channels, the scattering from any set of Bragg planes can be computed.

A. Bragg Reflections from a Mössbauer Crystal

For a single-Bragg reflection from a Mössbauer crystal, two channels will be open: the $t_0=(0+)$ channel, and a "reflection" channel r [Bragg case, shown in Fig. 2(c)], or a "transmission" channel t [Laue case, such as shown in Fig. 2(d)].

For a uniform Mössbauer crystal it is straightforward to obtain a general solution from Eqs. (33) and (34) for the polarization and amplitude of the reflected and transmitted waves by making the substitutions

$$\mathbf{T}_m{}^t=\sum_{k'}\mathbf{T}_{k'}{}^t e^{imk'd}\equiv\sum_{k'}\begin{pmatrix}T_{x,k'}{}^{(t)}\\ T_{y,k'}{}^{(t)}\end{pmatrix}e^{imk'd},$$

$$\mathbf{R}_m{}^r=\sum_{k'}\mathbf{R}_{k'}{}^r e^{imk'd}\equiv\sum_{k'}\begin{pmatrix}R_{x,k'}{}^{(r)}\\ R_{y,k'}{}^{(r)}\end{pmatrix}e^{imk'd}. \tag{35}$$

To be definite, we first assume that a reflection channel (r) is open, in addition to the t_0 channel. Substitution

of (35) into (33) and (34) gives

$$\begin{aligned}&[(e^{-i(g_0-k')d}-1)\tilde{I}-i\tilde{F}^{00}]\mathbf{T}_{k'}{}^{0}-i\tilde{F}^{0r}\mathbf{R}_{k'}{}^{r}=0,\\&-i\tilde{F}^{r0}\mathbf{T}_{k'}{}^{0}+[(e^{-i(g_r+k')d}-1)\tilde{I}-i\tilde{F}^{rr}]\mathbf{R}_{k'}{}^{r}=0,\end{aligned}\tag{36a}$$

and the boundary condition ($\lambda=x,y$),

$$\sum_{\lambda}\sum_{k'}T_{\lambda,k'}{}^{(0)}\boldsymbol{\varepsilon}_{\lambda}{}^{(0)}=\boldsymbol{\varepsilon}_0(\hat{k}_0,\omega_0),\tag{36b}$$

$$\sum_{k'}R_{\lambda,k'}{}^{(r)}e^{ik'M}=0.\tag{36c}$$

In (36a) $\tilde{I}$ is the 2×2 unit matrix. The dispersion equation to determine the allowed values of k' is then

$$\det\begin{pmatrix}(e^{-i(g_0-k')d}-1)\tilde{I}-i\tilde{F}^{00} & -i\tilde{F}^{0r}\\ -i\tilde{F}^{r0} & (e^{-i(g_r+k')d}-1)\tilde{I}-i\tilde{F}^{rr}\end{pmatrix}=0,\tag{37}$$

where the quantities with tildas are 2×2 matrices. Equation (37) gives four values of k' (which are independent of the basis of representation). There are then 16 amplitudes $T_{k',\lambda}{}^{(0)}$, $R_{k',\lambda}{}^{(r)}$ to be determined from the 16 linear relationships given by Eqs. (36a)–(36c). In particular, for a given value of k', the three independent equations (36a) give the determinant solutions

$$T_{y,k'}{}^{0}=D_{yx}{}^{00}(k')T_{x,k'}{}^{(0)},\quad R_{\lambda,k'}{}^{r}=D_{\lambda x}{}^{r0}(k')T_{x,k'}{}^{(r)}$$

in terms of $T_{x,k'}{}^{(0)}$. The four values of $T_{x,k'}{}^{(0)}$ are then determined from the boundary conditions (36b) and (36c), and the reflected and transmitted waves are then given by[38]

$$\mathbf{R}^{r}=\sum_{\lambda}\sum_{k'}\boldsymbol{\varepsilon}_{\lambda}{}^{(r)}R_{\lambda,k'}{}^{(r)},\tag{38a}$$

$$\mathbf{T}^{0}=\sum_{\lambda}\sum_{k'}\boldsymbol{\varepsilon}_{\lambda}{}^{(0)}T_{\lambda,k'}{}^{(0)}e^{ik'M}.\tag{38b}$$

The reflection and transmission coefficients are given by

$$R=g\int d\omega_0 d\hat{k}_0\frac{|\mathbf{R}^{r}|^{2}}{I_0},\quad T=\int d\omega_0 d\hat{k}_0\frac{|\mathbf{T}_0|^{2}}{I_0},\tag{39}$$

where

$$I_0=\int d\omega_0 d\hat{k}_0|\,\mathbf{a}_0(\omega_0,\hat{k}_0)|^{2},$$

$g=\sin\phi_1/\sin\phi_0$[Fig. 2(c)] is the Jacobian $|d^2(\hat{k}_0)/d^2(\hat{k}_1)|$, and the integration range is taken sufficiently small that the relative variation of g and ω_0 is negligible.

If a transmission channel t_1 is open instead of a reflection channel r, then the equations replacing (36a) are

$$\begin{aligned}&[(e^{-i(g_0-k')d}-1)\tilde{I}-i\tilde{F}^{00}]\mathbf{T}_{k'}{}^{0}-i\tilde{F}^{01}\mathbf{T}_{k'}{}^{1}=0,\\&-i\tilde{F}^{10}\mathbf{T}_{k'}{}^{0}+[(e^{-i(g_1-k')d}-1)\tilde{I}-i\tilde{F}^{11}]\mathbf{T}_{k'}{}^{1}=0,\end{aligned}\tag{40a}$$

and the boundary conditions are given by

$$\sum_{\lambda}\sum_{k'}T_{\lambda,k'}{}^{(0)}\boldsymbol{\varepsilon}_{\lambda}{}^{(0)}=\mathbf{a}_0(\omega_0,\hat{k}_0),\tag{40b}$$

$$\sum_{k'}T_{\lambda,k'}{}^{(1)}=0.\tag{40c}$$

In order to illustrate the general method of solving Eqs. (36) and (40), and to bring out certain features of the Mössbauer-Bragg scattering, we consider the limiting case, in which there is a well-defined quantization axis at each Mössbauer nucleus, which is perpendicular to the scattering plane (i.e., we assume that J_z is a good quantum number and that J_z is parallel to $\mathbf{k}_f\times\mathbf{k}_0$). For the "isotropic limit,"[39] of course, we can always take the quantization axis parallel to $\mathbf{k}_f\times\mathbf{k}_0$. It is easy to verify that in this case there is no orthogonal scattering if we use the following basis: $\boldsymbol{\varepsilon}_x{}^{(s)}(s=t_0,r)$ lies in the scattering plane, perpendicular to $\mathbf{k}_s$, and $\boldsymbol{\varepsilon}_y{}^{(s)}$ is taken perpendicular to the scattering plane such that $(\boldsymbol{\varepsilon}_x{}^{(s)},\boldsymbol{\varepsilon}_y{}^{(s)},\mathbf{k}_{(s)})$ forms a right-hand coordinate system. With this choice of basis there is no polarization mixing, and the four coupled linear equations of (36a) or (40a) separate into two sets of 2×2 coupled linear equations, one set containing only the x amplitudes and the second only the y amplitudes. In Secs. III A *i* and III A *ii* below, we examine the solutions for Bragg reflection and Laue transmission for this limiting case of no polarization mixing.[40]

(*i*) *Bragg reflection.* If the incident radiation is near a Bragg angle for a reflection channel r_1 as shown in Fig. 2(c), then

$$(g_0+g_1)d=2n\pi+2\delta.\tag{41}$$

We note that with g_0 and g_1 given by Eq. (25), Eq. (41) defines δ in terms of the angle of incidence ϕ_0. The dispersion equation then gives two values of $k_\lambda'(\lambda=x,y)$,

$$k_\lambda'=(g_0d-\delta+\alpha_\lambda\pm\beta_\lambda)/d,\tag{42a}$$

where

$$\alpha_\lambda=\tfrac{1}{2}(F_{\lambda\lambda}{}^{00}-F_{\lambda\lambda}{}^{11}),\tag{42b}$$

$$\beta_\lambda=[(\delta+\tfrac{1}{2}(F_{\lambda\lambda}{}^{00}+F_{\lambda\lambda}{}^{11}))^{2}-F_{\lambda\lambda}{}^{01}F_{\lambda\lambda}{}^{10}]^{1/2},\tag{42c}$$

and where the $F_{\lambda\lambda}{}^{ss'}$ are the planar scattering amplitudes defined by Eq. (32). In (42c), the square root is taken so that $I(\beta_\lambda)>0$.

The amplitude of the reflected $\boldsymbol{\varepsilon}_\lambda{}^{(1)}$ wave is then given by

$$R_\lambda(\delta,\omega)=\left(\frac{i\mathfrak{M}_\lambda F_{\lambda\lambda}{}^{10}}{1-i\mathfrak{M}_\lambda F_{\lambda\lambda}{}^{11}}\right)\boldsymbol{\varepsilon}_\lambda{}^{(0)*}\cdot\mathbf{a}_0(\omega,\hat{k}),\tag{43}$$

[38] Equation (38a) gives R_0, the reflected field *incident* on the first plane. The actual reflected wave can then be calculated from Eq. (33b), but the scattering effects of a single plane can generally be neglected. Similarly, (38b) actually gives T_M.

[39] By "isotropic limit" we mean the magnetically disordered state for which the splittings are negligible compared to Γ, e.g., Fe^{57} in stainless steel.

[40] The development given here is taken directly from the Ph.D. thesis of one of the authors (Ref. 14). Two recent papers by Afanas'ev and Kagan (Ref. 17) and O'Connor (Ref. 16) also treat the isotropic limit. Although there is some overlap of sections (A *i*, A *ii*) with these papers, different aspects are emphasized here and the approach is somewhat more general.

where $\mathfrak{M}_\lambda$ is given by

$$\mathfrak{M}_\lambda = \frac{1-e^{2iM\beta_\lambda}}{e^{-i(\delta+\alpha_\lambda+\beta_\lambda)}-1-e^{2iM\beta_\lambda}(e^{-i(\delta+\alpha_\lambda-\beta_\lambda)}-1)}. \tag{44}$$

For *thick crystals* such that $e^{iM\beta_\lambda}\approx 0$, then $\mathfrak{M}_\lambda \approx i(\delta+\alpha_\lambda+\beta_\lambda)^{-1}$, and

$$R_\lambda(\delta,\omega) = -\left(\frac{F_{\lambda\lambda}{}^{10}\boldsymbol{\varepsilon}_\lambda{}^{(0)*}\cdot\mathbf{a}_0(\omega,\hat{k})}{\delta+\frac{1}{2}(F_{\lambda\lambda}{}^{00}+F_{\lambda\lambda}{}^{11})+[(\delta+\frac{1}{2}(F_{\lambda\lambda}{}^{00}+F_{\lambda\lambda}{}^{11}))^2-F_{\lambda\lambda}{}^{01}F_{\lambda\lambda}{}^{10}]^{1/2}}\right), \tag{45}$$

which is the usual thick-crystal expression.[41] In the opposite limit of *thin films* (and very near Bragg), such that $|M\beta_\lambda|\ll 1$, then to terms of order $M^2\beta_\lambda{}^2$, $\mathfrak{M}_\lambda = M[1-iM(\delta+\alpha_\lambda)]^{-1}\simeq M$, the number of layers, and[42]

$$R_\lambda(\delta,\omega)\simeq iMF_{\lambda\lambda}{}^{10}\boldsymbol{\varepsilon}_\lambda{}^{(0)}\cdot\mathbf{a}_0(\omega,\hat{k})/[1-iM\delta-iM\tfrac{1}{2}(F_{\lambda\lambda}{}^{00}+F_{\lambda\lambda}{}^{11})]. \tag{46}$$

For the transmitted wave, the amplitude of the $\boldsymbol{\varepsilon}_\lambda{}^{(0)}$ component is given by

$$\begin{aligned} T_\lambda(\delta,\omega) &= \left[\left(\frac{e^{iM(\alpha_\lambda+\beta_\lambda)}}{1-i\mathfrak{M}_\lambda F_{\lambda\lambda}{}^{11}}\right)\left(\frac{e^{-i(\delta+\alpha_\lambda+\beta_\lambda)}-e^{-i(\delta+\alpha_\lambda-\beta_\lambda)}}{e^{-i(\delta+\alpha_\lambda+\beta_\lambda)}-1+e^{2iM\beta_\lambda}[e^{-i(\delta+\alpha_\lambda-\beta_\lambda)}-1]}\right)\boldsymbol{\varepsilon}_\lambda{}^{(0)}\cdot\mathbf{a}_0\right]e^{iM(g_0d-\delta)} \\ &\approx \left[\left(\frac{e^{iM(\alpha_\lambda+\beta_\lambda)}}{1-i\mathfrak{M}_\lambda F_{\lambda\lambda}{}^{11}}\right)\left(\frac{2\beta_\lambda}{\delta+\alpha_\lambda+\beta_\lambda-e^{2iM\beta_\lambda}(\delta+\alpha_\lambda-\beta_\lambda)}\right)\boldsymbol{\varepsilon}_\lambda{}^{(0)}\cdot\mathbf{a}_0\right]e^{iM(g_0d-\delta)}. \end{aligned} \tag{47}$$

One of the more interesting features of the dynamical solution is the suppression of the resonant absorption which occurs near a Bragg angle, as first pointed out by Trammell,[6] Muzikar,[7] and Afans'ev and Kagan.[11] That is, near a Bragg angle the integrated intensity of the reflected wave will generally maximize near resonance (although for small scattering angles from a thick crystal which contains a weak concentration of resonant atoms, a minimum can occur, as discussed below), and also the transmitted intensity, although minimizing near resonance, is generally much greater than the off-Bragg intensity. [This occurs because the transmitted intensity depends primarily on the $e^{iM\beta_\lambda}$ factor in (47), and β_λ, which depends on the square root of the difference between $\frac{1}{4}(F_{\lambda\lambda}{}^{00}+F_{\lambda\lambda}{}^{11})^2$ and $F_{\lambda\lambda}{}^{01}F_{\lambda\lambda}{}^{10}$, generally has a smaller imaginary part than $F_{\lambda\lambda}{}^{00}$, which determines the off-Bragg transmission.] The suppression of resonant absorption has been observed experimentally for both Bragg reflection[43] and Laue transmission.[44]

In order to illustrate this point, we consider the particularly simple case of an "isotropic" $M1$ Mössbauer transition and a simple cubic lattice containing a fraction E of the resonant nuclei. For further simplicity, we assume that the incident radiation is near Bragg for a symmetrical reflection (i.e., near a Bragg angle for the xy planes). For this case we have

$$\begin{aligned} &F_\lambda \equiv F_{\lambda\lambda}{}^{00} = F_{\lambda\lambda}{}^{11} = F_n + F_e, \\ &r_x \equiv F_{xx}{}^{10} = F_{xx}{}^{01} = F_n + r_e\cos(2\phi_0), \\ &r_y \equiv F_{yy}{}^{10} = F_{yy}{}^{01} = F_n\cos(2\phi_0) + r_e, \end{aligned} \tag{48a}$$

where $(2\phi_0)$ is the scattering angle (ϕ_0 is the angle of incidence with respect to the xy planes), and

$$\begin{aligned} F_n &= \frac{2\pi\lambda_0{}^2ndE[\exp(-k_0{}^2\langle x^2\rangle)]\Gamma_\gamma}{(2J_0+1)\sin\phi_0\,(\Delta E - k_0 - i\frac{1}{2}\Gamma)}, \\ F_e &= \frac{\lambda_0 nd(-Zr_0+ik_0\sigma_e/4\pi)}{\sin\phi_0}, \\ r_e &= \frac{\lambda_0 nd\,\exp(-\frac{1}{2}\langle[(\mathbf{k}_f-\mathbf{k}_0)\cdot\mathbf{x}]^2\rangle)[-F(2\phi_0)r_0+ik_0\sigma_e/4\pi]}{\sin\phi_0}. \end{aligned} \tag{48b}$$

F_e and r_e in (48b) should, of course, be the coherent average of the Mössbauer and non-Mössbauer atoms. For a numerical estimate we take an iron crystal containing 65% Fe^{57}. Then for $\boldsymbol{\varepsilon}_x$ polarized resonant radiation incident at exact Bragg (with $E/\sin\phi = 1$), we have $T\sim 0.04$, $R\sim 0.67$; while off Bragg, $T\sim 2\times 10^{-4}$ and $R\sim 2\times 10^{-7}$. This is for $M\approx 10^4$.

This suppression of resonant absorption near Bragg can be viewed as due to an enhanced coherent scattering

[41] In comparing with the standard results, e.g., Ref. 3, p. 428, note that the $|\gamma_m|$, $|\gamma_0|$ factors which appear in the x-ray results for unsymmetrical reflection are the same as the $\sin\phi_{(s)}$ factors which are included in the $F_{\lambda\lambda}{}^{ss'}$.

[42] The discrepancy between Eq. (47) and Eq. (27) of Ref. 17 arises from the neglect of the planar self-action in the present treatment.

[43] P. J. Black and P. W. Moon, Nature **188**, 481 (1960).

[44] V. K. Voitovetskii, I. L. Korsunskii, and Yu. F. Pazhin, Zh. Eksperim. i Teor. Fiz. Pis'ma v Redaktsiyu **8**, 611 (1968) [English transl.: Soviet Phys.—JETP Letters **8**, 377 (1968)].

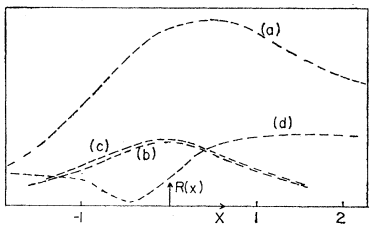

FIG. 3. Curves showing the form of the integrated intensity $R(x)$ of the reflected wave as a function of the source velocity for a thick simple-cubic iron crystal containing Fe^{57} for (a) $\phi_0=10°$, $E=0.65$, (b) $\phi_0=45°$, $E=0.65$, (c) $\phi_0=60°$, $E=0.65$, and (d) $\phi_0=10°$, $E=0.02$.

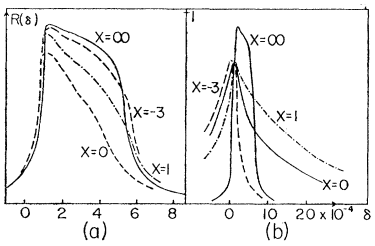

FIG. 4. Curves showing the reflected intensity $R(\delta)$ as a function of $\delta=k_0 d\sin\phi\ \delta\phi$, the deviation from Bragg, for different frequencies $x=2(k_0-\Delta E)/\Gamma$ for a thick simple-cubic iron crystal containing Fe^{57}. In (a), $E=0.02$, and in (b), $E=0.65$.

width. For a highly enriched crystal for which we can neglect F_e, r_e with respect to F_n near resonance, we have in the thin-crystal limit

$$|R_{x,y}|^2=\left|\left(\frac{2\pi M\Gamma_{\rm coh}}{k_0^2d^2\sin\phi_0}\right)(1,\cos2\phi_0)\Big/\left[\Delta E-k_0-i\tfrac{1}{2}\left(\Gamma+\frac{2\pi M\Gamma_{\rm coh}}{k_0^2d^2\sin\phi_0}\right)\right]\right|^2, \quad (49)$$

where $\Gamma_{\rm coh}=E\exp(-k_0^2\langle x^2\rangle)\,(2J_0+1)^{-1}\Gamma_\gamma$. From this form we see that the coherent scattering width of the system is enhanced by

$$\Gamma_{\rm crystal}=(2\pi M\Gamma_{\rm coh}/k_0^2d^2\sin\phi_0). \quad (50)$$

The width is proportional to the number of layers, and can be much greater than the radiative width Γ_γ for an isolated nucleus (for the idealized case considered above, $\Gamma_{x1}\sim1.5\times10^2\Gamma_\gamma$). For sufficiently large M, Γ_{x1} dominates Γ_α, the width for absorptive processes, and there is a corresponding enhancement of the coherent elastic scattering and a suppression of the absorptive processes. This enhancement of the coherent width at Bragg angles and suppression of the absorptive processes was first pointed out by Trammell[6] and Muzikar,[7] and corresponds to the Dicke's superradiant emission states.[45] The coherent width for emission of a photon from a crystal is also given by (50) as shown by these authors and by Zaretskii and Lomonosov.[46] It is interesting to note that, since the lifetime is inversely proportional to the width, a photon incident at a Bragg angle escapes from the crystalline system faster than from an isolated nucleus.

Experimentally, of course, one is interested in the integrated intensities. In Fig. 3 we plot the integrated intensity of the reflected wave, $R(v_s)$, as a function of the source velocity for the case considered above of a symmetric Bragg reflection from a thick, simple cubic crystal of Fe^{57} in iron at room temperature. The source is assumed unpolarized, with a beam collimation of 2×10^{-3} rad.

[45] R. H. Dicke, Phys. Rev. **93**, 99 (1954).

[46] D. F. Zaretskii and V. V. Lomonosov, Zh. Eksperim. i Teor. Fiz. **48**, 368 (1965) [English transl.: Soviet Phys.—JETP **21**, 243 (1965)].

The curves labeled (a)–(c) in Fig. 3 give $R(v_s)$ for a highly enriched crystal for the angles of incidence $\phi=10°$, 45°, and 60°. For these cases the intensity maximizes near resonance. As discussed by Black, Evans, Longworth, Moon, and O'Connor, the frequency asymmetry and the displacement of the maximum from resonance is due to the interference between the Rayleigh and the resonant nuclear scattering.[43,47–50] For the isotropic $M1$ case being considered, this interference term is proportional to $R(r_eF_n^*\cos2\phi)$, and for $\phi<45°$ the region of constructive interference is shifted to the high-frequency side ($k_0>\Delta E$), for $\phi>45°$, to the low-frequency side, and for $\phi=45°$ there is no interference. The most pronounced interference effects occur for the small scattering angles, where the electronic scattering amplitude is of comparable magnitude to the nuclear scattering amplitude. For the large scattering angles the interference effects are almost negligible because the electronic scattering amplitude is greatly decreased by the phonon and form factors [for $\phi_0=60°$, $F(2\phi)/F(0)\simeq0.17$, and $f_D(2\phi)\simeq0.5$].

The curve 3(d) gives $R(v_s)$ for $\phi_0=10°$, $E=0.02$, and for this case the intensity minimizes near resonance.[51] This behavior is also obtained near grazing incidence (see Sec. III C and Fig. 5), where $R(v_s)$ minimizes near resonance if the angle of incidence of the beam is less than the critical angle ϕ_c, while a maximum is obtained if the angle of incidence is greater than ϕ_c.

A qualitative insight into the dependence of the resonance behavior of $R(v_s)$ upon the beam collimation, the angle of incidence, and the fraction E of Mössbauer atoms is obtained by examining the angular dependence of $|R_\lambda(\delta,\omega)|^2$. In Figs. 4(a) and 4(b) we plot $|R_x(\delta,\omega)|^2$ as a function of δ for $E=0.02$, 0.65, and $\phi=10°$.

The curves labeled $x=\infty$ are the purely electronic scattering curves. As is well known, the reflected intensity for this case has a region of near total reflection

[47] P. B. Moon, Proc. Roy. Soc. (London) **A263**, 309 (1961).

[48] P. J. Black, D. E. Evans, and D. A. O'Connor, Proc. Roy. Soc. (London) **A270**, 168 (1962).

[49] P. J. Black, G. Longworth, and D. A. O'Connor, Proc. Phys. Soc. (London) **83**, 925 (1964); **83**, 937 (1964).

[50] D. A. O'Connor and P. J. Black, Proc. Phys. Soc. (London) **83**, 941 (1964).

[51] In Ref. 49, the conditions for obtaining a maximum or a minimum near resonance are discussed from the kinematical viewpoint.

for $-R(F_\lambda-r_\lambda)<\delta<-R(F_\lambda+r_\lambda)$, where F_λ and r_λ are given by Eq. (49) with $F_n=0$.

In Fig. 4(a), the crystal has a weak concentration of Mössbauer atoms, $E=0.02$. For this case $F_n\sim 1.1\times10^{-4}\times(x-i)^{-1}$ while $F_e\sim-6.1\times10^{-4}+i2.0\times10^{-5}$ and $r_e\sim-3.3\times10^{-4}+i2.0\times10^{-5}$. Thus even at resonance, the dominant contributions to the coherent scattering amplitudes are the real parts of F_e and r_e, and the region of maximum scattering is still contained within the region $\delta\propto-R(F_e\pm r_e)$. As the frequency of the incident radiation nears the resonance frequency, F_n is primarily imaginary and acts as an absorptive contribution to F_e and r_e. As shown in Fig. 4(a), the intensity within the maximum scattering region is strongly decreased, and it is clear that the integrated intensity will exhibit a minimum in the resonance region.

In Fig. 4(b), E is taken as 0.65, for which $F_n\sim3.5\times10^{-3}(x-i)^{-1}$, and F_n gives the dominant contribution to the scattering amplitudes near resonance. For this case the region of strong scattering is greatly broadened near resonance, with a maximum spread on the order of $|F_n|_{k_0=\Delta E}$. It is this broadening of the scattering region that gives a maximum to the integrated intensity such as shown in Figs. 3(a)–3(c). Of course, within the region $\delta\propto R(F_e\pm r_e)$, $|R(\delta,\omega)|^2$ as a function of frequency again strongly decreases near resonance, so that if the incident beam were collimated to this region, a minimum would always occur. Except near grazing incidence, however, such a collimation generally cannot be obtained experimentally (for the case being considered, this would correspond to an angular collimation $\sim4\times10^{-4}$ rad).

Qualitatively then, the reflected wave will maximize near resonance if $\langle\delta\rangle>|F_n|_{x=0}>|r_e|$, i.e., the most favorable conditions for a maximum are for highly enriched crystals, large scattering angles, and uncollimated radiation [or collimated radiation lying outside of the region $\delta\propto R(F_e\pm r_e)$].[51]

Finally, we note that polarization can be important. For example, in the simple case considered above, $R_x(v_s)$ will always minimize near resonance for a Bragg angle of $\phi=45°$. This occurs because $\cos(2\phi)=0$, so that the numerator only contains r_e and is frequency-independent, while the denominator contains F_n and maximizes at resonance. The physical reason for this is that for $\phi=45°$ and incident $\boldsymbol{\varepsilon}_x$, the magnetic dipoles vibrate in the direction of the reflected wave and hence do not contribute to the scattered field, and the reflected wave is caused by electronic scattering. However, the reflected wave from a layer will interact with the magnetic dipoles in upper layers, and this interaction dissipates energy from the reflected wave.

(ii) Laue transmission. If the incident radiation is near a Bragg angle for a transmission channel τ_1 as shown in Fig. 2(d), then

$$(g_0-g_1)d=2n\pi+2\delta\,, \tag{51}$$

and the dispersion equation gives ($\lambda=x,y$)

$$k_\lambda'=(g_0d-\delta+\alpha_\lambda\pm\beta_\lambda)\,, \tag{52a}$$

where for the Laue case,

$$\alpha_\lambda=\tfrac{1}{2}(F_{\lambda\lambda}{}^{00}+F_{\lambda\lambda}{}^{11})\,, \tag{52b}$$

$$\beta_\lambda=\{[\delta+\tfrac{1}{2}(F_{\lambda\lambda}{}^{00}-F_{\lambda\lambda}{}^{11}]^2+F_{\lambda\lambda}{}^{01}F_{\lambda\lambda}{}^{10}\}^{1/2}. \tag{52c}$$

The square root is again taken so that $I(\beta_\lambda)>0$.

The amplitude for the $\boldsymbol{\varepsilon}_\lambda{}^{(1)}$ component of the wave with $\mathbf{k}_1=(g_1,\mathbf{k}_{xy}{}^0+\boldsymbol{\tau}_{xy}{}^1)$ wave is then given by

$$T_\lambda{}^1(\delta,\omega)=[-\boldsymbol{\varepsilon}_\lambda{}^{(0)}\cdot\mathbf{a}_0iF^{10}\sin M\beta_\lambda\, e^{i(M-1)\alpha_\lambda}/\sin\beta_\lambda]\times e^{iM(g_0d-\delta)-i\delta}\,, \tag{53}$$

and the $\boldsymbol{\varepsilon}_\lambda{}^{(0)}$ component of the k_0 wave is given by

$$T_\lambda{}^0(\delta,\omega)=\{\boldsymbol{\varepsilon}_\lambda{}^{(0)}\cdot\mathbf{a}_0[\cos M\beta_\lambda+i\nu_\lambda\sin M\beta_\lambda/\sin\beta_\lambda]\times e^{iM\alpha_\lambda}\}e^{iM(g_0d-\delta)}\,, \tag{54}$$

where

$$i\nu_\lambda=[1+iF_{\lambda\lambda}{}^{00}-\tfrac{1}{2}(e^{-i(\delta-\alpha_\lambda-\beta_\lambda)}+e^{-i(\delta-\alpha_\lambda+\beta_\lambda)})]e^{i(\delta-\alpha_\lambda)}\approx i[\delta+\tfrac{1}{2}(F_{\lambda\lambda}{}^{00}-F_{\lambda\lambda}{}^{11})]e^{i(\delta-\alpha_\lambda)}. \tag{55}$$

From Eqs. (53) and (54) we see that, for a thin film, very near Bragg, $T_\lambda{}^{(1)}\approx iMF_{\lambda\lambda}{}^{10}$ and $T_\lambda{}^{(0)}\approx(1+iM\alpha_\lambda)$. As a function of frequency, the $\mathbf{k}_1$ wave in this case will exhibit a maximum in the region of constructive interference between the electronic and nuclear scattering, while the $\mathbf{k}_0$ wave exhibits a weak minimum.

For a thick film the dominant contributions to $T_\lambda{}^{(1)}$ and $T_\lambda{}^{(0)}$ come from the exponential term depending on the difference between α_λ and β_λ, i.e.,

$$T_\lambda{}^{(1)}(\delta,\omega)\simeq-\tfrac{1}{2}\boldsymbol{\varepsilon}_\lambda{}^{(0)}\cdot\mathbf{a}_0(F_{\lambda\lambda}{}^{10}/\beta_\lambda)e^{iM(\alpha_\lambda-\beta_\lambda)}\,,$$
$$T_\lambda{}^{(0)}(\delta,\omega)\simeq\tfrac{1}{2}\boldsymbol{\varepsilon}_\lambda{}^{(0)}\cdot\mathbf{a}_0(1-\nu_\lambda/\beta_\lambda)e^{iM(\alpha_\lambda-\beta_\lambda)}\,. \tag{56}$$

Since the imaginary part of $\alpha_\lambda-\beta_\lambda$ will generally maximize in the resonance region, it is clear that as a function of frequency, both the τ_0 and τ_1 waves will exhibit a minimum in the resonance region for a thick film (and it is only for the thin-film limit discussed above that a maximum will occur). Of course, the total transmitted intensity is still much greater than for the off-Bragg case.[44]

B. Off-Bragg Transmission through a Mössbauer Medium

Off Bragg, to a very good approximation, we only need consider the (0+) channel open. This channel only involves the forward scattering amplitudes, and the optical solutions are thus valid for a noncrystalline medium, as well as for a crystal.

As pointed out in Ref. 14, there are two, generally nonorthogonal, frequency-dependent eigenwaves in a Mössbauer medium, which have different complex indexes of refraction.[52] This gives rise to a number of interesting optical effects, such as a Faraday effect,

[52] A different approach to this problem is given by Blume and Kistner in Ref. 15.

and allows selective absorption or selective critical reflection of the eigenwaves.

(*i*) *Eigenwaves in a uniform Mössbauer medium.* Setting $R_{\lambda,k'}{}^{(r)}\equiv 0$ in (36a) and taking

$$e^{i(k'-g_0)d}=(1+if_\eta d/\sin\phi_0), \tag{57}$$

then the eigenpolarizations and indexes of refraction are determined by the eigenvalue equation

$$\begin{pmatrix} f_{xx} & f_{xy} \\ f_{yx} & f_{yy} \end{pmatrix}\begin{pmatrix} T_{x,k'} \\ T_{y,k'} \end{pmatrix}=f_\eta\begin{pmatrix} T_{x,k'} \\ T_{y,k'} \end{pmatrix}, \tag{58}$$

where f_{xx}, etc., are the planar forward-scattering amplitudes defined by (32) and again we have used $\boldsymbol{\varepsilon}_x$, $\boldsymbol{\varepsilon}_y$ to denote *any* two *orthogonal* polarizations perpendicular to $\mathbf{k}_0$.

From (58) we obtain (for $\eta=1,2$)

$$f_\eta=\tfrac{1}{2}(f_{xx}+f_{yy})+(-1)^{\eta+1}\times[\tfrac{1}{4}(f_{xx}-f_{yy})^2+f_{xy}f_{yx}]^{1/2}, \tag{59}$$

where the square root is taken to have a positive imaginary part. The corresponding eigenpolarizations $\boldsymbol{\varepsilon}_\eta$ are given by[53]

$$\boldsymbol{\varepsilon}_\eta(\hat{k},\omega)=K_{(\eta,x)}[\boldsymbol{\varepsilon}_x+(f_\eta-f_{xx})/f_{xy}\boldsymbol{\varepsilon}_y], \tag{60}$$

where

$$K_{(\eta,x)}=[1+|(f_\eta-f_{xx})/f_{xy}|^2]^{-1/2}. \tag{61}$$

From (57) we see that $k_\eta'd=g_0d+f_\eta d/\sin\phi_0+O(f_\eta d)^2$, so that within the medium the $\boldsymbol{\varepsilon}_\eta$ eigenwave decreases (to first order) as $e^{-If_\eta t}$, and the corresponding index of refraction is given by

$$n_\eta=1+\chi_0 f_\eta. \tag{62}$$

We note that since the scattering matrix in (58) is not generally Hermitian,[54] the eigenwaves $\boldsymbol{\varepsilon}_\eta$ are generally nonorthogonal. Only in the limiting cases of well-isolated resonances, "isotropic" resonances, off resonance, or, if J_z is a good quantum number, for $\hat{k}_0\cdot\hat{z}=0,\ \pm1$, will the eigenwaves be strictly orthogonal. (Orthogonality can also be obtained in some cases for propagation along a high symmetry axis of the crystal, as discussed by Housley, Grant, and Gonser[55]). Although it is not immediately obvious, it can be verified that f_η and $\boldsymbol{\varepsilon}_\eta$ are invariant with respect to the choice of orthogonal basis, as they must be. We also note that the eigenpolarizations are functions of $\mathbf{k}$, ω, so that each component of an incident packet has different eigenwaves.

(*ii*) *Transmission through a Mössbauer medium.* The polarization and intensity of the coherent, elastic wave transmitted through a Mössbauer medium is easily obtained using the exponentially decaying eigenwaves (60). The polarization and amplitude of the $(\mathbf{k},\omega)$ component of the incident photon we write as

$$\mathbf{a}_0(\hat{k},\omega)=K(\omega,\hat{k})[\alpha(\omega,\hat{k})\boldsymbol{\varepsilon}_x(\hat{k})+\beta(\omega,\hat{k})\boldsymbol{\varepsilon}_y(\hat{k})], \tag{63}$$

where $\boldsymbol{\varepsilon}_x(\hat{k})$ and $\boldsymbol{\varepsilon}_y(\hat{k})$ are an orthogonal polarization basis perpendicular to the momentum vector $\mathbf{k}$ of the incident photon, and K, α, β are complex functions of $(\hat{k},\omega)$ with the normalization

$$I_0=\int d\omega d\hat{k}\,|\mathbf{a}_0|^2=\int d\omega d\hat{k}\,|K|^2(|\alpha|^2+|\beta|^2), \tag{64}$$

where I_0 is the intensity of the incident packet. If the incident photon is unpolarized, then $\beta\propto e^{i\psi}$, where ψ is an arbitrary phase angle, and there is an additional $\int(d\psi/2\pi)$ integration in Eq. (64).

$\mathbf{a}_0(\hat{k},\omega)$ can be expressed in terms of the exponentially decaying eigenwaves $\boldsymbol{\varepsilon}_\eta(k,\omega)$ by

$$\begin{aligned}\boldsymbol{\varepsilon}_x&=a_x\boldsymbol{\varepsilon}_{(1)}+b_x\boldsymbol{\varepsilon}_{(2)},\\ \boldsymbol{\varepsilon}_y&=a_y\boldsymbol{\varepsilon}_{(1)}+b_y\boldsymbol{\varepsilon}_{(2)},\end{aligned} \tag{65}$$

where

$$\begin{aligned}a_x&=(f_1-f_{yy})/[(f_1-f_2)K_{(1,x)}],\\ b_x&=-(f_2-f_{yy})/[(f_1-f_2)K_{(2,x)}].\end{aligned} \tag{66}$$

a_y and b_y are given by Eq. (66) by interchanging all x and y subscripts. The $(\mathbf{k},\omega)$ component of the wave transmitted through a Mössbauer medium of thickness t (where t is thickness along the direction of propagation) is then given by

$$\mathbf{T}(\mathbf{k},\omega)=K(\alpha a_x+\beta a_y)e^{if_1t}\boldsymbol{\varepsilon}_{(1)}+K(\alpha b_x+\beta b_y)e^{if_2t}\boldsymbol{\varepsilon}_{(2)}, \tag{67}$$

or, in terms of the orthogonal basis $\boldsymbol{\varepsilon}_x(\mathbf{k})$, $\boldsymbol{\varepsilon}_y(\mathbf{k})$,

$$\mathbf{T}(\hat{k},\omega)=K\left\{\tfrac{1}{2}\alpha e_{(+)}+e_{(-)}\left[-\tfrac{1}{2}\alpha\left(\frac{f_{xx}-f_{yy}}{f_1-f_2}\right)+\beta\left(\frac{f_{xy}}{f_1-f_2}\right)\right]\right\}\boldsymbol{\varepsilon}_x+K\left\{\tfrac{1}{2}\beta e_{(+)}+e_{(-)}\left[\tfrac{1}{2}\beta\left(\frac{f_{yy}-f_{xx}}{f_1-f_2}\right)+\alpha\left(\frac{f_{yx}}{f_1-f_2}\right)\right]\right\}\boldsymbol{\varepsilon}_y, \tag{68}$$

where

$$e_{(\pm)}=e^{if_1t}\pm e^{if_2t}. \tag{69}$$

A phase factor $e^{ig_0t\sin\phi_0}$ has been taken into the factor K in Eqs. (67) and (68).

[53] There are, of course, a number of alternative forms for ϵ_η which are obtained by using the determinant equation of (58), i.e., $(f_{xx}-f_\eta)(f_{yy}-f_\eta)-f_{xy}f_{yx}=0$, and by modifying the factor $K_{(\eta,x)}$. In particular, we can interchange all x and y subscripts in (60) and (61). In going from one basis to another, over-all phase factors are absorbed into $K_{(\eta,x)}$.

[54] See, for example, Blume and Kistner, Ref. 15.

[55] R. M. Housley, R. W. Grant, and U. Gonser, Phys. Rev. **178**, 514 (1969).

The intensity of the transmitted packet is given by

$$I=\int\frac{d\psi}{2\pi}\int d\omega d\hat{k}\,|\mathbf{T}(\hat{k},\omega)|^2=I_x+I_y, \tag{70}$$

where

$$I_x=\int\frac{d\psi}{2\pi}\int d\omega d\hat{k}\,|K|^2\left\{\tfrac{1}{4}|\alpha e_+|^2+|e_-|^2\left|\tfrac{1}{2}\alpha\left(\frac{f_{xx}-f_{yy}}{f_1-f_2}\right)+\beta\left(\frac{f_{xy}}{f_1-f_2}\right)\right|^2\right.$$
$$\left.+\tfrac{1}{2}e^*_{(+)}e_{(-)}\left[\tfrac{1}{2}|\alpha|^2\left(\frac{f_{xx}-f_{yy}}{f_1-f_2}\right)+\beta\alpha^*\left(\frac{f_{xy}}{f_1-f_2}\right)\right]+\text{c.c.}\right\}, \tag{71a}$$

$$I_y=\int\frac{d\psi}{2\pi}\int d\omega d\hat{k}\,|K|^2\left\{\tfrac{1}{4}|\beta e_+|^2+|e_-|^2\left|\tfrac{1}{2}\beta\left(\frac{f_{yy}-f_{xx}}{f_1-f_2}\right)+\alpha\left(\frac{f_{yx}}{f_1-f_2}\right)\right|^2\right.$$
$$\left.+\tfrac{1}{2}e_{(+)}e^*_{(-)}\left[\tfrac{1}{2}|\beta|^2\left(\frac{f_{yy}-f_{xx}}{f_1-f_2}\right)+\alpha\beta^*\left(\frac{f_{yx}}{f_1-f_2}\right)\right]+\text{c.c.}\right\}. \tag{71b}$$

If the incident packet is unpolarized, then $\beta/\alpha\propto e^{i\psi}$, and the terms $\alpha\beta^*$, $\alpha^*\beta$ in Eqs. (71a) and (71b) give no contribution.

When the composition and unit-cell internal field structures are known, Eq. (68) gives the amplitude and polarization of the transmitted wave in terms of any convenient orthogonal basis, and (71) gives the intensity of the components. Conversely, if the internal field structure is unknown, these expressions can be used to obtain information about the internal field parameters by carrying out polarization experiments (i.e., polarized source line, and/or measurement of intensities of transmitted components $\boldsymbol{\varepsilon}_x$, $\boldsymbol{\varepsilon}_y$ by using polarizing filter. See for example Housley, Grant, and Gonser[55]).

When the frequency distribution and spread of the incident photon packet is specified, the integrations in (71) can be carried out analytically (in some cases) to give the explicit dependence on the thicknesses of the source and absorber. Except for the simplest cases, however, these expressions are generally quite complicated.[56]

As given by Eq. (67), the transmitted wave $\mathbf{T}(\hat{k},\omega)$ is a superposition of the exponentially damped eigenwaves $\boldsymbol{\varepsilon}_1$, $\boldsymbol{\varepsilon}_2$. Since the indexes of refraction of the two waves are different, i.e.,

$$n_{(1)}-n_{(2)}=2\chi_0\{[\tfrac{1}{4}(f_{xx}-f_{yy})]^2+f_{xy}f_{yx}]^{1/2}, \tag{72}$$

there are Faraday effects involved in the transmission through a Mössbauer medium. The real part of $n_{(1)}-n_{(2)}$ gives the usual Faraday rotation effect, while the imaginary gives a "selective absorption" effect. Since the electronic scattering gives no contribution to (72) (in the limit that we have treated $E_{\mu\nu}$), $n_{(1)}-n_{(2)}$ depends only upon the nuclear scattering amplitude and will be primarily imaginary at resonance, while the real part will dominate off-resonance. Thus at resonance the Faraday effect in Mössbauer optics is primarily one of selective absorption. That is, if the resonances are well separated and if the incident frequency (packet) is within a few widths of a resonance, so that $I(f_1)\gg I(f_2)$, then the $\boldsymbol{\varepsilon}_1$ eigenwave will be damped out much more rapidly. For such a case, the thickness t of the polarizing medium can be chosen sufficiently thick so that almost all of the $\boldsymbol{\varepsilon}_1$ wave is absorbed, but still sufficiently thin such that the $\boldsymbol{\varepsilon}_2$ wave is only slightly attenuated, and the transmitted wave is nearly $\boldsymbol{\varepsilon}_2$ polarized. In particular, selective absorption of the eigenwaves gives a means for obtaining a (partially) polarized, monochromatic Mössbauer beam for scattering or absorption experiments, and a means for measuring the intensity of a particular polarization of a Mössbauer beam. In order to obtain a well-polarized beam it is necessary that $I(f_1)\gg I(f_2)$. It is obvious that to satisfy this condition requires strong Zeeman splitting within the polarizing medium, and, furthermore, the imaginary part of the nuclear scattering amplitude must be much greater than the imaginary part of the electronic scattering amplitude. Because of the rapid decrease of the Mössbauer phonon factor with increasing k_0, the second condition is only well satisfied for the low-energy Mössbauer transitions. For a high-energy transition such as the 90-keV Ru^{99} transition, only weak partial polarization can be obtained by selective absorption even at low temperatures.

When $\mathbf{T}(\hat{k},\omega)$ is expressed in terms of an orthogonal basis $\boldsymbol{\varepsilon}_x$, $\boldsymbol{\varepsilon}_y$ as given by Eq. (68), the contribution

$$e_{(+)}+e_{(-)}\left(\frac{f_{xx}-f_{yy}}{f_1-f_2}\right)$$

to the $\boldsymbol{\varepsilon}_x$ component of the transmitted wave includes the effects of the absorption of $\boldsymbol{\varepsilon}_x$ within the medium and the decrease in the $\boldsymbol{\varepsilon}_x$ amplitude due to the orthogonal

[56] S. Margulis and J. R. Ehrman, Nucl. Instr. Methods **12**, 131 (1961).

scattering $\boldsymbol{\varepsilon}_x \rightarrow \boldsymbol{\varepsilon}_y$ within the medium. The final term, $e_{(-)}f_{xy}/(f_1-f_2)$, gives the increase (or decrease, depending on the phase) in the $\boldsymbol{\varepsilon}_x$ amplitude due to the orthogonal scattering $\boldsymbol{\varepsilon}_y \rightarrow \boldsymbol{\varepsilon}_x$.

C. Grazing Incidence

If the incident photon is near grazing incidence with respect to the xy planes, then all the scattering matrices $\tilde{F}^{(ss')}(s, s'=0, r)$ in Eqs. (36a) and (36b) can be taken equal to the forward-scattering matrix $\tilde{F}^{(00)}$ to order ϕ (where ϕ is the angle of grazing incidence). In this approximation, then, the matrices can all be simultaneously diagonalized, and the equations separate into two sets of Darwin-Prins equations as in the special cases considered in Sec. III A *i*. It is clear that the diagonalizing bases are the nonorthogonal eigenwaves $\boldsymbol{\varepsilon}_\eta(\hat{k}_0,\omega), \boldsymbol{\varepsilon}_\eta(\hat{k}_r,\omega)$ defined by Eq. (60), since

$$2\pi\lambda_0 n M_{\mu\nu}(\mathbf{k}_{(s')},\mathbf{k}_{(s)})[\boldsymbol{\varepsilon}_\eta(\hat{k}_{(s)},\omega)]_\nu = f_\eta([\boldsymbol{\varepsilon}_\eta(\hat{k}_{(s')},\omega)]_\mu + O(\phi)), \quad (s, s'=0, r)$$

where f_η is given by Eq. (59).

The Darwin-Prins solutions given in Sec. III A *i* can then be used, with the appropriate modifications for the nonorthogonality of the bases. In particular, for an incident $\boldsymbol{\varepsilon}_0 = \boldsymbol{\varepsilon}_\eta(\mathbf{k}_0,\omega)$ photon, the reflected wave is given by Eq. (45), which after some manipulation becomes

$$\mathbf{R}(\hat{k}_r,\omega) = R_\eta \boldsymbol{\varepsilon}_\eta(\hat{k}_r,\omega), \tag{73a}$$

$$R_\eta = \frac{1-(1+2\lambda f_\eta/\phi^2)^{1/2}}{1+(1+2\lambda f_\eta/\phi^2)^{1/2}}. \tag{73b}$$

For the special cases for which the eigenbases are orthogonal, the reflected wave for an incident photon of arbitrary polarization is given by

$$\mathbf{R}(\hat{k}_r,\omega) = \sum_{\eta=1,2} R_{(\eta)}(\boldsymbol{\varepsilon}_0 \cdot \boldsymbol{\varepsilon}_\eta^*)\boldsymbol{\varepsilon}_\eta.$$

For the general case where the $\boldsymbol{\varepsilon}_\eta$ are nonorthogonal, we adopt the following convention: $\boldsymbol{\varepsilon}_\eta(\hat{k}_0,\omega)$ is analyzed in terms of an arbitrary orthogonal basis $\boldsymbol{\varepsilon}_x(\hat{k}_0), \boldsymbol{\epsilon}_y(\hat{k}_0)$ as given by Eq. (60), and $\boldsymbol{\varepsilon}_\eta(\mathbf{k}_r,\omega)$ in terms of $\boldsymbol{\varepsilon}_x(\hat{k}_r)$, $\boldsymbol{\varepsilon}_y(\hat{k}_r)$, where $\boldsymbol{\varepsilon}_\lambda(\hat{k}_r)$ $(\lambda = x,y)$ is obtained from $\boldsymbol{\varepsilon}_\lambda(\hat{k}_0)$ by a rotation of 2ϕ about the $\hat{k}_r \times \hat{k}_0$ axis. Then if the $(\mathbf{k}_0,\omega)$ component of the incident photon is $\mathbf{a}_0(\hat{k}_0,\omega) = K(\hat{k}_0,\omega)[\alpha\boldsymbol{\varepsilon}_x(\mathbf{k}) + \beta\boldsymbol{\varepsilon}_y(\mathbf{k})]$, the reflected $(\hat{k}_r,\omega)$ component is (to order ϕ)

$$\mathbf{R}(\mathbf{k}_r,\omega) = K[(\alpha a_x + \beta a_y)R_1\boldsymbol{\varepsilon}_1(\mathbf{k}_r,\omega) + (\alpha b_x + \beta b_y)R_2\boldsymbol{\varepsilon}_2(\mathbf{k}_r,\omega)], \tag{74}$$

where a_x, b_x, a_y, b_y are defined in Eq. (66). In terms of the orthogonal bases, (74) becomes

$$\mathbf{R}(\hat{k}_r,\omega) = K\left\{\tfrac{1}{2}\alpha R_{(+)} + R_{(-)}\left[\tfrac{1}{2}\alpha\left(\frac{f_{xx}-f_{yy}}{f_1-f_2}\right) + \beta\left(\frac{f_{xy}}{f_1-f_2}\right)\right]\right\}\boldsymbol{\varepsilon}_x(\mathbf{k}_r) + K\left\{\tfrac{1}{2}\beta R_{(+)} + R_{(-)}\left[\tfrac{1}{2}\beta\left(\frac{f_{yy}-f_{xx}}{f_1-f_2}\right) + \alpha\left(\frac{f_{yx}}{f_1-f_2}\right)\right]\right\}\boldsymbol{\varepsilon}_y(\hat{k}_r), \tag{75}$$

where

$$R_{(\pm)} = R_1 \pm R_2. \tag{76}$$

We note that Eqs. (74)–(76) are directly analogous to the transmission formulas, Eqs. (67)–(69).

In Fig. 5 we plot $|R(\hat{k}_r,\omega)|^2$ as a function of ϕ for a highly enriched ($E=0.55$) film of Fe^{57} in stainless steel, for several different frequencies. Off resonance there is a region of near total reflection for $\phi < \phi_c = [-2\lambda\,\mathrm{Re}(f_e)]^{1/2} \approx 3.8\times10^{-3}$ rad. In the resonance region, there is no true critical angle, owing to the large absorption, but a rough characterization of the curves is given by the frequency-dependent "critical angle" $\phi_\eta(\omega) = [-2\lambda\,\mathrm{Re}(f_\eta(\omega))]^{1/2}$. In Fig. 5, the positions of the $\phi_\eta(\omega)$ are indicated by crosses. The region $\phi < \phi_\eta(\omega)$ is a region of strong scattering for a wave of frequency ω. As a function of frequency, $\phi_\eta(\omega)$ maximizes for $\omega = \Delta E + \frac{1}{2}\Gamma$ ($x=+1$ in Fig. 5), i.e., at the frequency of maximum constructive interference between the Rayleigh and nuclear scattering, and the ϕ region of strong reflection is much broader than for off resonance. Similarly, if $|\mathrm{Re}(f_\eta(\omega))| < |\mathrm{Re}(f_e)|$ for all ω, then $\phi_\eta(\omega)$ has a minimum for $\omega = \Delta E - \frac{1}{2}\Gamma$, the frequency of maximum destructive interference between the Rayleigh and nuclear scattering, and the region of strong scattering is much smaller than for off resonance. For the case considered in Fig. 5, $\phi_\eta(\omega)$ is not defined for $\omega \approx \Delta E - \frac{1}{2}\Gamma$ [i.e., $\phi_\eta(\omega)$ is imaginary], but the intensity curves for $\phi_\eta(\omega)$ undefined also have very small regions of strong scattering with respect to off resonance.

From Fig. 5 it is clear that if the incident beam is collimated so that $\phi_0 - \delta\phi < \phi < \phi_0 + \delta\phi < \phi_c$, then as a function of frequency the reflected intensity will exhibit a sharp minimum in the low-frequency side of the

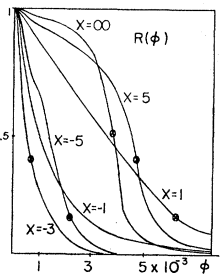

FIG. 5. Curves showing the reflected intensity near grazing incidence as a function of ϕ for different frequencies $x = 2(k_0 - \Delta E)/\Gamma$ for a highly enriched ($E=0.55$) film of Fe^{57} in stainless steel. The crosses indicate the position of $\phi_\eta(x)$.

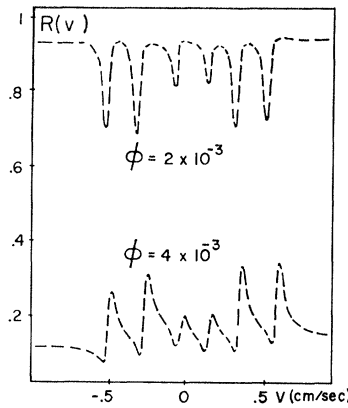

FIG. 6. Curves showing the reflected intensity as a function of the source velocity grazing incidence ($\phi_0=2\times10^{-3}$ rad and $\phi_0=4\times10^{-3}$ rad) from a film of 90% Fe^{57} in iron, which is magnetically ordered by a field $\mathbf{H}\perp\mathbf{k}_0$, $\mathbf{H}$ in the plane of the film.

resonance. In terms of the frequency-dependent critical angle $\phi_\eta(\omega)$, the minimum occurs when $\phi_\eta(\omega)$ becomes less than $\phi_0-\delta\phi$, i.e., when the (fixed) angle of incidence becomes greater than the frequency-dependent critical angle. Similarly if $\phi_0-\delta\phi>\theta_c$, the reflected intensity will have a maximum on the high-frequency side of the resonance, where $\phi_\eta(\omega)$ maximizes.

Returning to the general case of nonisotropic resonances, where the reflected wave amplitude is given by Eqs. (74)–(76), we note selective critical reflection of the eigenwaves is possible. If the resonances are well separated and if the incident frequency is within a few widths of a resonance so that $I(f_{(1)})\gg I(f_{(2)})$, then the $|R_{(1)}|^2$ reflection amplitude [Eq. (73b)] of the $\boldsymbol{\varepsilon}_{(1)}$ eigenwave has a frequency and angular dependence similar to the near-resonant reflected intensity curves shown in Fig. 5, while the $|R_{(2)}|^2$ amplitude varies slowly with frequency, and as a function of ϕ behaves similarly to the nonresonant ($x=\infty$) curve of Fig. 5. Thus, if the incident collimation is $\phi_0-\delta\phi<\phi<\phi_0+\delta\phi<\phi_c$, and if the incident frequency is Doppler-shifted so that $\omega_0\approx\Delta E-\frac{1}{2}\Gamma$, then the $\boldsymbol{\varepsilon}_{(1)}$ eigenwave will be only weakly reflected while the $\boldsymbol{\varepsilon}_{(2)}$ wave is almost totally reflected. Similarly if $\phi_0-\delta\phi>\phi_c$, then for $\omega_0\approx\Delta E+\frac{1}{2}\Gamma$, the $\boldsymbol{\varepsilon}_{(1)}$ eigenwave will be strongly reflected and $\boldsymbol{\varepsilon}_{(2)}$ will be only weakly reflected.

As a particular example, we consider the 14.4-keV γ ray from a source of Fe^{57} in stainless steel at grazing incidence on a film of 90% Fe^{57} in iron which is magnetically oriented by a field $\mathbf{H}\perp\mathbf{k}_0$, $\mathbf{H}$ in the plane of the film. This problem has been investigated by Bernstein and Campbell.[10] Off resonance, the critical angle is $\phi_c=3.4\times10^{-3}$ rad.[57] In Figs. 6(a) and 6(b), we give the reflected intensity as a function of frequency for $\phi_0=4\times10^{-3}$ rad and $\phi_0=2\times10^{-3}$ rad (and a uniform spread of $\delta\phi_0=0.5\times10^{-3}$). For $\phi_0=4\times10^{-3}$ rad (2×10^{-3}), 13% (93%) reflection occurs off resonance. At frequency of the maximum (minimum) of scattering near the $|\frac{3}{2},\frac{3}{2}\rangle\leftrightarrow|\frac{1}{2},\frac{1}{2}\rangle$ resonance, the ε_x component of the Mössbauer packet ($\boldsymbol{\varepsilon}_x\perp$ to the plane of the film) has a reflection coefficient ≈0.55 (0.21), while for the ε_y component of the Mössbauer packet, and for the nonrecoilless part of the 14.4-keV radiation, the reflection coefficient is ≈0.13 (0.93). The 123- and 137-keV background radiation is almost completely removed, the reflection coefficient being on the order of 10^{-4}.

As a means for obtaining partially polarized, unsplit Mössbauer beams selective critical reflection offers two advantages over selective absorption: the Mössbauer intensity can be enhanced relative to the non-Mössbauer intensity, and it is unnecessary to have carefully prepared polarizing filters of a precise thickness. Selective critical reflection has the disadvantage, however, of requiring well-collimated incident radiation (and owing to the collimation problems, this technique appears to be applicable only to low-energy Mössbauer transitions), and generally the degree of polarization of the Mössbauer beam is not as great.

APPENDIX A

In this Appendix we give a short discussion of the derivation of the single-atom resonant scattering operator $N_{\mu\nu}^{(i)}$ along modern lines. We include the effects of lattice vibrations and give a brief discussion of the modifications which occur when relaxation effects are important.

Wigner and Weiskopf's[58] derivation of the resonance dispersion formula is well known. More general modern discussions of radiation damping formulations may be found in the text books by Heitler[59] and Goldberger and Watson.[60]

We suppose that the initial photon's energy ω_0 is very near a nuclear resonance energy. In this case the second graph of Fig. 7(a) is negligible, and it is only the sum of the contributions of the first graph of Fig. 7(a) with that of Figs. 7(b) and 7(c) and the higher iterates which are important (initially we assume that we are dealing with a bare nucleus). The sum of the contributions of these graphs to the scattered photon potential is

$$(A_\mu{}^s(x))^{f0}=\langle\phi_f\chi_f|-i\int\delta_+(x-x')e^{iH_0t'}J_\mu(\mathbf{x}')G(t'-t'')\times J_\nu(\mathbf{x}'')A_\nu{}^0(x'')e^{-iH_0t''}dx'dx''|\phi_0\chi_0\rangle, \quad \text{(A1)}$$

where G is the propagator including electromagnetic self-action in the ladder approximation, and is given by the

[57] We have taken $F(2\phi)=21.6$ to fit the off-resonance data of Ref. 10.

[58] V. Weisskopf and E. Wigner, Z. Physik **63**, 54 (1930); **65**, 18 (1930).

[59] W. Heitler, *Quantum Theory of Radiation* (Oxford University Press, London, 1954), pp. 163–174.

[60] M. L. Goldberger and K. M. Watson, *Collision Theory* (John Wiley & Sons, Inc., New York, 1964), pp. 424–509.

Dyson equation,

$$G=G_0-iG_0J\delta_{(+)}G_0JG_0+(-i)^2G_0J\delta_{(+)}G_0JG_0J\delta_{(+)}G_0JG_0+\cdots$$
$$=G_0-iG_0J\delta_{(+)}G_0JG. \quad \text{(A2)}$$

In Eq. (A2), G_0 is the uncorrected propagator given by

$$G_0(t-t')=1(t-t')e^{-iH_0(t-t')}, \quad \text{(A3)}$$

where H_0 is the Hamiltonian for the nucleus plus crystal with the electromagnetic interaction represented by instantaneous Coulomb interactions.

The matrix notation of (A1) and (A2) is explained by writing (A2) out explicitly,

$$G(t_1-t_4)=G_0(t_1-t_4)-i\int G_0(t_1-t_2)J_\mu(\mathbf{x}_2)\delta_{(+)}(x_2-x_3)$$
$$\times G_0(t_2-t_3)J_\mu(\mathbf{x}_3)G(t_3-t_4)dx_2dx_3, \quad \text{(A2')}$$

where the integrations are over all space-time. However, since G_0 only progagates into the future, effectively $t_1>t_2>t_3>t_4$. Writing

$$\tilde{G}(\omega)=\int_{-\infty}^{+\infty}e^{i\omega t}G(t)dt$$

for the Fourier transform (ω assumed to have infinitesimal positive imaginary part), the transform of (A2') gives

$$\tilde{G}(\omega)=\tilde{G}_0-i\tilde{G}_0\tilde{\Delta}\tilde{G} \quad \text{(A4a)}$$

or

$$\tilde{G}=(1+i\tilde{G}_0\tilde{\Delta})^{-1}\tilde{G}_0, \quad \text{(A4b)}$$

where Δ in Eqs. (A4a) and (A4b) is given by

$$\Delta=J\delta_{(+)}G_0J. \quad \text{(A5)}$$

If $|\varphi_n\rangle|\chi_n\rangle$ is an eigenfunction of H_0 [where the χ and ϕ notation is that used in Eq. (2)] it can easily be shown by the methods of Paper I that Δ, and hence G, is diagonal in the χ_n's. [If $\mathbf{r}(t)$ is the c.m. operator, $J\delta_+G_0J$ involves $e^{i\mathbf{k}\cdot\mathbf{r}(t)}\delta_+(\mathbf{k},t-t')e^{-i\mathbf{k}\cdot\mathbf{r}(t')}$. The important contribution from $\delta_+(\mathbf{k},t-t')$ comes from $(t-t')$ on the order of the time for a photon to traverse the nucleus. Thus, to a very good approximation, we can set $t=t'$, and this operator becomes independent of $\mathbf{r}(t)$.] G is also diagonal in the φ_n's except for very unimportant radiative correction effects. $\tilde{\Delta}$ then commutes with H_0, and using $G_0(\omega)=i/(\omega-H_0)$, we obtain the well-known expression,

$$\tilde{G}(\omega)=i/[\omega-H_0-\tilde{\Delta}(\omega)]. \quad \text{(A6)}$$

The real part of the level shift operator $\Delta(\omega)$ is of no concern to us. After subtracting the effect of the instantaneous Coulomb interactions and the electromagnetic self-energies there is left only a very small radiation correction to the nuclear level which is quite negligible. We are then only concerned with the imaginary portion of $\tilde{\Delta}(\omega)=-i\frac{1}{2}\Gamma(\omega)$.

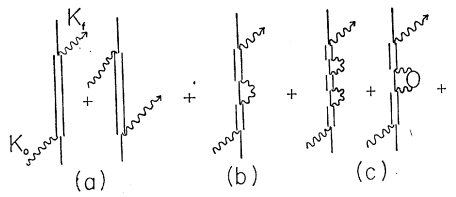

FIG. 7. Feynman diagrams representing contributions to the nuclear scattering operator $T(J_\mu(x)J_\nu(y))$.

For many Mössbauer transitions the decay takes place predominantly via internal conversion rather than γ-ray emission. The radiation reaction on the nucleus due to this process is represented by adding the contribution of the second graph of Fig. 7(c). In this graph the closed loop represents the promotion of an electron in a normally filled atomic level to above the Fermi surface and its eventual return to its initial state. The effect of this is to add to (A5), which we will now call Δ_γ, a term Δ_α (α is the usual symbol for the internal conversion coefficient),

$$\Delta=\Delta_\gamma+\Delta_\alpha,$$
$$\Delta_\gamma=J\delta_{(+)}G_0J, \quad \text{(A7)}$$
$$\Delta_\alpha=J\delta_{(+)}E\delta_{(+)}G_0J, \quad \text{(A8)}$$

where E is the electronic scattering operator.

Taking the Fourier transform and matrix element of (A7) we have

$$\langle\phi_n\chi_0|\tilde{\Delta}_\gamma(\omega)|\phi_n\chi_0\rangle=-4\pi\int\frac{d^4k}{(2\pi)^4}\int dt\,e^{i(\omega-E_a-\epsilon_0)t}$$
$$\times\sum_a J_\mu{}^{na}(\mathbf{k})J_\mu{}^{an}(-\mathbf{k})\left(\frac{e^{ik_4t}}{k_4{}^2-\mathbf{k}\cdot\mathbf{k}+i\epsilon}\right)\langle e^{i\mathbf{k}\cdot\mathbf{r}(t)}e^{-i\mathbf{k}\cdot\mathbf{r}(t')}\rangle. \quad \text{(A9)}$$

As previously noted, the bracketed expression, which represents the nuclear-motion propagator during the exchange of the virtual quanta, may be set equal to 1. For the imaginary part of (A9) we may extend the time integral to $-\infty$, and we then obtain the well-known expression for the radiative width of the level $|\phi_n\rangle$,

$$-\tfrac{1}{2}i\Gamma_\gamma(k_\omega)=\mathrm{Im}\int d\mathbf{x}d\mathbf{y}\sum_a J_\mu{}^{na}(\mathbf{x})\frac{e^{ik_\omega|\mathbf{x}-\mathbf{y}|}}{|\mathbf{x}-\mathbf{y}|}J_\mu{}^{an}(\mathbf{y}). \quad \text{(A10)}$$

In (A10), $k_\omega=\omega-E_a-\epsilon_0$. When the time integrations are carried out in (A1) the resulting Fourier transforms are evaluated at $\omega=\omega_0+E_a+\epsilon_0$, for which $k_\omega=k_0$.

Similarly, for the imaginary part of (A8) we have

$$-\tfrac{1}{2}i\Gamma_\alpha(k_\omega)=\mathrm{Im}\int d\mathbf{r}_1d\mathbf{r}_2d\mathbf{x}d\mathbf{y}$$
$$\times\sum_a J_\mu{}^{na}(r_2)\frac{e^{ik_\omega|\mathbf{r}_2-\mathbf{x}|}}{|\mathbf{r}_2-\mathbf{x}|}E_{\mu\nu}{}^{(0)}(\mathbf{x},\mathbf{y})\frac{e^{ik_\omega|\mathbf{y}-\mathbf{r}_1|}}{|\mathbf{y}-\mathbf{r}_1|}J_\nu{}^{an}(\mathbf{r}_1), \quad \text{(A11)}$$

where

$$E_{\mu\nu}{}^{(0)}(\mathbf{x},\mathbf{y})=\sum_{k,p}\left(\frac{j_\mu{}^{kp}(\mathbf{x})j_\nu{}^{pk}(\mathbf{y})}{k_\omega-E_p+E_k+i\eta}+\frac{j_\mu{}^{pk}(\mathbf{x})j_\nu{}^{kp}(\mathbf{y})}{-k_\omega-E_p+E_k+i\eta}\right) \quad \text{(A12)}$$

is the electronic scattering operator, to the first order in e^2. In (A12) $j_\mu(\mathbf{x})$ is the electronic current operator and k is to be summed over the normally filled states (energies E_k), p over the normally unoccupied states (E_p).

Strictly, Eq. (A11) contains in addition to the nuclear damping due to internal conversion, a correction to (A10). The correction term is small and the dominant contribution to (A11) is that arising from the pole in the electronic scattering operator.

Returning to (A1) and carrying out the time integrations (and using the slow-collision time assumption) leads directly to Eq. (2).[61]

When relaxation effects are important, it is convenient to write Eq. (2) in the form

$$A_\mu{}^s(z)=\frac{e^{i(k_0|z-R_i{}^0|-\omega_0\tau_z)}}{|\mathbf{z}-\mathbf{R}_i{}^0|}\left[-i\int_0^\infty dt\, e^{(i\omega_0 t-\frac{1}{2}\Gamma t)}\langle\langle\chi_0\phi_0|e^{-ik_f\cdot r_i(t)}G_0{}^+(t)J_\mu(-\mathbf{k}_f)G_0(t)J_\nu(\mathbf{k}_0)e^{ik_0-r_i}|\phi_0\chi_0\rangle\rangle\right]A_\nu(\mathbf{R}_i{}^0), \quad \text{(A13)}$$

where $\Gamma=\Gamma_\gamma+\Gamma_\alpha$ is the total width of the near resonant excited sublevels. Here we are concerned only with the coherent elastically scattered wave, and the brackets $\langle\,\rangle$ indicate that the ensemble average is to be taken. The quantity in square brackets gives $\langle N_{\mu\nu}(\mathbf{k}_f,\mathbf{k}_0)\rangle$. To calculate the resonance response of the scattering operator it is necessary to calculate the current-current correlation function.

Equation (A13) is directly analogous to the correlation function formulations for Mössbauer absorption or emission spectra in the presence of relaxation phenomena, such as developed by Afanas'ev and Kagan,[62,63] Bradford and Marshall,[64] and Blume and Tjon,[65,66] and the same methods of solving for the correlation function can be applied here.

It is beyond the scope of this paper to attempt a general discussion of the effect of relaxation phenomena on Mössbauer resonance scattering, but we note that in analogy to the absorption and emission problems, the resonance response of $N_{\mu\nu}$ is only a simple Breit-Wigner response in the fast-relaxation limit (static "effective field" limit). When the relaxation time is on the order of the Larmor precession time of the excited nuclear state, the resonances can be shifted or split, the effective widths can be broadened or narrowed, and lines corresponding to normally forbidden transitions can be obtained (the latter feature, however, can also be obtained in the fast-relaxation limit, as discussed in Appendix C).

APPENDIX B

For reference, we summarize the basic multipole formulas used in Secs. II A and II C. The notation is that of Akhiezer and Berestetskii.[28]

The multipole expansions of the current operators $J(\mathbf{x})e^{i|\mathbf{z}-\mathbf{x}|}/|\mathbf{z}-\mathbf{x}|$, and $J(\mathbf{x})e^{\pm i\mathbf{k}\cdot\mathbf{x}}$, are given by (for $|z|>|x|$)

$$J(\mathbf{x})\frac{e^{ik|\mathbf{z}-\mathbf{x}|}}{|\mathbf{z}-\mathbf{x}|}=\frac{ik}{4\pi}\sum_L\sum_{M=-L}^{L}\left[J_4(\mathbf{x})\phi_{LM}{}^*(\mathbf{x})\Phi_{LM}(\mathbf{z}),\right.$$
$$\left.\sum_{\lambda=-1}^{+1}\mathbf{J}(\mathbf{x})\cdot\mathbf{A}_{LM}{}^{(\lambda)}(\mathbf{x})^*\,\mathbf{B}_{LM}{}^{(\lambda)}(\mathbf{z})\right] \quad \text{(B1)}$$

and

$$J(\mathbf{x})e^{-ik\cdot x}=\sum_{L,M}\left[J_4(\mathbf{x})\phi_{LM}{}^*(\mathbf{x})Y_{LM}(\hat{k}),\right.$$
$$\left.\sum_{\lambda=-1}^{+1}\mathbf{J}(\mathbf{x})\cdot\mathbf{A}_{LM}{}^{(\lambda)}(\mathbf{x})^*\,\mathbf{Y}_{LM}{}^{(\lambda)}(\hat{k})\right]. \quad \text{(B2)}$$

The scalar and vector potentials are given by

(i) $\phi_{LM}(\mathbf{x})=g_L(kx)Y_{LM}(\hat{\mathbf{x}})$ (B3)

$$\mathbf{A}_{LM}{}^{(1)}(\mathbf{x})=\mathbf{Y}_{LM}{}^{(1)}(\hat{\mathbf{x}})[Lg_{L+1}(kx)+(L+1)g_{L-1}(kx)]\times(2L+1)^{-1}+\mathbf{Y}_{LM}{}^{(-1)}(\hat{\mathbf{x}})\times[g_{L-1}(kx)-g_{L+1}(kx)](L^2+L)^{1/2}\times(2L+1)^{-1},$$

$$\mathbf{A}_{LM}{}^{(0)}(\mathbf{x})=g_L(kx)\mathbf{Y}_{LM}{}^{(0)}(\hat{\mathbf{x}}),$$

$$\mathbf{A}_{LM}{}^{(-1)}(\mathbf{x})=\mathbf{Y}_{LM}{}^{(-1)}(\hat{\mathbf{x}})[Lg_{L-1}(kx)+(L+1)g_{L+1}(kx)]\times(2L+1)^{-1}+\mathbf{Y}_{LM}{}^{(1)}(\mathbf{x})\times[g_{L-1}(kx)-g_{L+1}(kx)]\times(L^2+L)^{1/2}(2L+1)^{-1},$$

[61] We have omitted consideration of the second-order Doppler shift pointed out by B. D. Josephson [Phys. Rev. Letters 4, 341 (1960)] and by R. V. Pound and G. A. Revka, Jr. [*ibid.* 4, 274 (1960)]. The intermediate phonon states should actually be taken as x_n', where x_n' corresponds to x_n, but with the mass of the excited nucleus increased by $\hbar\omega_0/c^2$. The denominator in Eq. (2) then contains the additional term $\epsilon_0-\epsilon_0'$, which gives the second-order Doppler-shift effect for resonant scattering.

[62] A. M. Afanas'ev and Yu. Kagan, Zh. Eksperim. i Teor. Fiz. 45, 1660 (1963) [English transl.: Soviet Phys.—JETP 18, 1139 (1964)].

[63] Yu. Kagan and A. M. Afanas'ev, Zh. Eksperim. i Teor. Fiz. 47, 1108 (1964) [English transl.: Soviet. Phys.—JETP 20, 743 (1965)].

[64] E. Bradford and W. Marshall, Proc. Phys. Soc. (London) 87, 731 (1966).

[65] M. Blume and J. A. Tjon, Phys. Rev. 165, 446 (1968).

[66] M. Blume, Phys. Rev. 174, 351 (1968).

where $g_L(kx)$ is the spherical Bessel function

$$g_L(z)=4\pi(i)^L(\pi/2z)^{1/2}J_{L+1/2}(z). \quad \text{(B4)}$$

The expressions for Φ_{LM} and $B_{LM}{}^{(\lambda)}$ are given by (B3) with the replacement $g_L \rightarrow G_L$, where G_L is the spherical Hankel function of the first kind,

$$G_L(z)=4\pi(i)^L(\pi/2z)^{1/2}H_{L+1/2}{}^{(1)}(z). \quad \text{(B5)}$$

The components of the vector spherical harmonics $\mathbf{Y}_{LM}{}^{(\lambda)}$ along the unit vector $\hat{\mathbf{e}}_r$, $\hat{\mathbf{e}}_\theta$, $\hat{\mathbf{e}}_\phi$ of spherical polar coordinates are given by

$$(Y_{LM}{}^{(-1)})_r=Y_{LM}, \quad \text{(B6a)}$$

$$(Y_{LM}{}^{(-1)})_\phi=(Y_{LM}{}^{(-1)})_\theta=0, \quad \text{(B6b)}$$

$$(Y_{LM}{}^{(1)})_r=(Y_{LM}{}^{(0)})_r=0, \quad \text{(B6c)}$$

$$(Y_{LM}{}^{(1)})_\theta=i(Y_{LM}{}^{(0)})_\phi=[L(L+1)]^{-1/2}\times(\partial Y_{LM}/\partial\theta), \quad \text{(B6d)}$$

$$(Y_{LM}{}^{(1)})_\phi=-i(Y_{LM}{}^{(0)})_\theta=[L(L+1)]^{-1/2}(\sin\theta)^{-1}\times(\partial Y_{LM}/\partial\phi). \quad \text{(B6e)}$$

The transverse vector spherical harmonics $\mathbf{Y}_{LM}{}^{(1)}(\hat{\mathbf{k}})$, $\mathbf{Y}_{LM}{}^{(0)}(\hat{\mathbf{k}})$ are related to the circularly polarized bases $\boldsymbol{\eta}_{(\pm1)}(\hat{\mathbf{k}})$ transverse to $\mathbf{k}$ by

$$\left(\frac{8\pi}{2L+1}\right)^{1/2}\mathbf{Y}_{LM}{}^{(\lambda)}(\hat{\mathbf{k}})=\boldsymbol{\eta}_{(1)}(\mathbf{k})\,\mathfrak{D}_{1,M}{}^{(L)}(\hat{\mathbf{k}},\hat{z})+(-1)^{(\lambda+1)}\boldsymbol{\eta}_{(-1)}(\hat{\mathbf{k}})\mathfrak{D}_{1,M}{}^{(L)}(\hat{\mathbf{k}},\hat{z}), \quad \text{(B7)}$$

where the notation for the rotation matrices $\mathfrak{D}$ is that of Rose.[22]

For $\lambda=0$, 1, the matrix elements

$$\left[\int d\mathbf{x}\,\mathbf{J}(\mathbf{x})\cdot\mathbf{A}_{LM}{}^{(\lambda)}(\mathbf{x})\right]^{na}$$

and

$$\left[\int d\mathbf{x}\,\mathbf{J}(\mathbf{x})\cdot\mathbf{A}_{LM}{}^{(\lambda)}(\mathbf{x})^*\right]^{a'n}$$

are easily evaluated in terms of the radiative width $\Gamma_\gamma(L,\lambda)$, i.e., the width associated with the emission of (L,λ)-multipole radiation. [The ratio of the radiative widths gives the mixing ratio δ^2, i.e., $\delta^2(E2/M1)=\Gamma_\gamma(E2)/\Gamma_\gamma(M1)$.] Denoting the spin of the states explicitly, $|a\rangle=|a,J_a,m_a\rangle$ and $|n\rangle=|n,J_n,m_n\rangle$, we have

$$\langle a|\int d\mathbf{x}\,J(\mathbf{x})\cdot\mathbf{A}_{LM}{}^{(\lambda)}(\mathbf{x})^*|n\rangle=\delta_{M,m_n-m_0}C(J_0LJ_n;m_0Mm_n)|\chi(L,\lambda)|e^{i\eta L^\lambda}, \quad \text{(B8)}$$

where $\chi(L,\lambda)$ is the reduced matrix element for the transition. Substituting (B2) into the width expression

$$\Gamma_\gamma(k_0)=-\lambda_0{}^{-1}\sum_a\int d\hat{\Omega}\,J_\mu{}^{na}(k_0\hat{\Omega})J_\mu{}^{an}(-k_0\hat{\Omega}),$$

we obtain

$$\Gamma_\gamma=\sum_{L,\lambda=0,1}\Gamma_\gamma(L,\lambda)=\lambda_0{}^{-1}\sum_{L,\lambda=0,1}|\chi(L,\lambda)|$$

or

$$\chi(L,\lambda)=[\lambda_0\Gamma_\gamma(L,\lambda)]^{1/2}. \quad \text{(B9)}$$

APPENDIX C

The multipole-scattering amplitudes given by Eq. (4) are only valid in the fast-relaxation limit and only if J_z is conserved for the nucleus. Here we discuss the modifications (for the fast-relaxation limit) when J_z is not conserved, because of an asymmetric EFG tensor (or even an axially symmetric EFG tensor if the symmetry axis is noncoaxial with H).

The asymmetry terms will mix the states of good J_z, and the eigenstates for the level $|\alpha_n,J_n\rangle$ are given by

$$|\alpha_n,J_n,\mu_n\rangle=\sum_{m_n}K(\mu_n,m_n)|n,J_n,m_n\rangle. \quad \text{(C1)}$$

The index μ_n takes on the same values as m_n, and the $K(\mu_n,m_n)$ are the elements of the appropriate unitary transformation matrix. The (L,λ) multipole component of current matrix elements for emission then becomes

$$\langle 0|\sum_M\mathbf{Y}_{LM}{}^{(\lambda)}(\hat{\mathbf{k}})\int d\mathbf{x}\,\mathbf{J}(\mathbf{x})\cdot\mathbf{A}_{LM}{}^{(\lambda)}(\mathbf{x})^*|n\rangle=[\lambda_0\Gamma_\gamma(L,\lambda)]^{1/2}e^{i\eta L^\lambda}\sum_M\mathbf{Y}_{LM}{}^{(\lambda)}(\hat{\mathbf{k}})G_{LM}(\mu_n\mu_0), \quad \text{(C2)}$$

where

$$G_{LM}(\mu_n\mu_0)=(-1)^M\sum_{m_0}K(\mu_n,M+m_0)K^*(\mu_0,m_0)\times C(J_nLJ_0;m_n-Mm_0). \quad \text{(C3)}$$

The scattering amplitude is then given by Eq. (2), with the replacements

$$\mathbf{Y}_{L'M'}{}^{(\lambda')}(\hat{\mathbf{k}}_f)\rightarrow\sum_{M'}\mathbf{Y}_{L'M'}{}^{(\lambda')}(\hat{\mathbf{k}}_f)G_{L'M'}(\mu_n\mu_0), \quad \text{(C4a)}$$

$$\mathbf{Y}_{LM}{}^{(\lambda)}(\hat{k}_0)^*\rightarrow\sum_M\mathbf{Y}_{LM}{}^{(\lambda)}(\hat{\mathbf{k}}_0)^*G_{LM}{}^*(\mu_n\mu_0), \quad \text{(C4b)}$$

$$x(m_0M)\rightarrow x(\mu_0\mu_n)=2[E(J_n,\mu_n)-E(J_0,\mu_0)-k_0]/\Gamma. \quad \text{(C4c)}$$

The effect of the induced electronic currents is still given by Eq. (15).

For a pure (L,λ) multipole transition, the polarization of an emitted photon is now a mixture of the vector spherical harmonics $\mathbf{Y}_{LM}{}^{(\lambda)}(\hat{\mathbf{k}}_f)$, as given by (C4a), and owing to the state mixing, there are more allowed transitions than for the J_z conserved case.

As a simple example we consider a $J_0=\frac{1}{2}\rightarrow J_n=\frac{3}{2}$ $M1$ transition where the effective Hamiltonian of the nucleus is given by

$$\mathfrak{H}=\mathfrak{H}_0+\hat{g}\beta HJ_z+\hat{Q}[3J_z{}^2-J^2+\tfrac{1}{2}\eta(J_+{}^2+J_-{}^2)]. \quad \text{(C5)}$$

For the $j_0=\frac{1}{2}$ ground state, J_z is still conserved and the eigenstates are $|\alpha_0, \frac{1}{2}, \pm\frac{1}{2}\rangle$, while for the excited level, the states are given by

$$\begin{pmatrix} |\frac{3}{2}, \quad \mu=\frac{3}{2}\rangle \\ |\frac{3}{2}, \quad \mu=\frac{1}{2}\rangle \\ |\frac{3}{2}, \mu=-\frac{1}{2}\rangle \\ |\frac{3}{2}, \mu=-\frac{3}{2}\rangle \end{pmatrix} = \begin{pmatrix} A_{3/2} & 0 & A_{3/2}\epsilon_{3/2} & 0 \\ 0 & A_{1/2} & 0 & A_{1/2}\epsilon_{1/2} \\ A_{-1/2}\epsilon_{-1/2} & 0 & A_{-1/2} & 0 \\ 0 & A_{-3/2}\epsilon_{-3/2} & 0 & A_{-3/2} \end{pmatrix} \times \begin{pmatrix} |\frac{3}{2},\frac{3}{2}\rangle \\ |\frac{3}{2},\frac{1}{2}\rangle \\ |\frac{3}{2}, -\frac{1}{2}\rangle \\ |\frac{3}{2}, -\frac{3}{2}\rangle \end{pmatrix}, \quad \text{(C6)}$$

where

$$\epsilon_{\pm 3/2}=\{[(3Q\pm Z)^2+3Q^2\eta^2]^{1/2}-(3Q\pm Z)\}/Q\eta\sqrt{3}, \quad \text{(C7a)}$$

$$\epsilon_{\pm 1/2}=-\epsilon_{\mp 3/2}, \quad \text{(C7b)}$$

$$A_\lambda=(1+\epsilon_\lambda^2)^{-1/2}, \quad \text{(C7c)}$$

where $Z=g\beta H$. We note that $\epsilon_\lambda \to 0$ as $\eta \to 0$.

Thus, the polarization for a photon emitted by the $|\frac{3}{2}, \mu=\frac{3}{2}\rangle \to |\frac{1}{2},\frac{1}{2}\rangle$ transition, which would be $\propto \mathbf{Y}_{11}^{(0)}(\mathbf{k})$ for J_z conserved, now contains an admixture of $\mathbf{Y}_{1-1}^{(0)}$, i.e., the polarization is proportional to

$$[C(\tfrac{3}{2}, 1, \tfrac{1}{2}; \tfrac{3}{2}, -1, \tfrac{1}{2})\mathbf{Y}_{1-1}^{(0)}(\hat{\mathbf{k}}) + \epsilon_{3/2}C(\tfrac{3}{2}, 1, \tfrac{1}{2}; -\tfrac{1}{2}, 1, \tfrac{1}{2})\mathbf{Y}_{1-1}^{(0)}(\mathbf{k})].$$

For the $|\frac{3}{2}, \mu=\frac{3}{2}\rangle \to |\frac{1}{2}, -\frac{1}{2}\rangle$ transition, which is not allowed for J_z conserved, the amplitude and polarization of the emitted photon is proportional to $[\epsilon_{3/2}C(\frac{3}{2}, 1, \frac{1}{2}; -\frac{1}{2}, 0, -\frac{1}{2})\mathbf{Y}_{10}^{(0)}(\mathbf{k})]$.

APENDIX D

In this Appendix we give a brief discussion of an alternative formulation of Mössbauer optics, which is essentially an extension of the Laue theory of x-ray optics.

In I, we found that if a photon $A_\mu^0(\mathbf{R},t)$ is incident on a Mössbauer medium the total coherent wave is given by [Eqs. (50)–(51) or (53) of I]

$$A_\mu(\mathbf{R},t)=A_\mu^0(\mathbf{R},t)+\sum \frac{e^{ik_0|\mathbf{R}-\mathbf{R}_j^0|-i\omega_0 t}}{|\mathbf{R}-\mathbf{R}_j^0|} \times M_{\mu\nu}(\mathbf{k},\mathbf{k}')A_\nu^j(\mathbf{R}_j^0), \quad \text{(D1)}$$

where $\mathbf{R}_j^0$ is the equilibrium position of the jth atom, $\mathbf{k}=-i\overleftarrow{\nabla}_{\mathbf{R}_j^0}$, $\mathbf{k}'=-i\vec{\nabla}_{\mathbf{R}_j^0}$, and $M_{\mu\nu}(\mathbf{k},\mathbf{k}')$ is the coherent elastic scattering operator (for simplicity we first assume that $M_{\mu\nu}$ is independent of $\mathbf{R}_j$). The field $A_\nu^i(\mathbf{R}_i^0)$ is the coherent field incident on the $\mathbf{R}_i$th site and is given by (D1) with the $j=i$ term deleted, i.e., $A_\nu^j(\mathbf{R}_j^0)$ is equal to the total coherent field at $\mathbf{R}_j^0$ with the singular self-field deleted. The superscript j can be deleted with the understanding that $A_\nu(\mathbf{R})$ at a lattice site $\mathbf{R}=\mathbf{R}_j$ excludes the self-field of the jth scatterer. The self-field effects (e.g., the radiative width and energy level shifts) are included in the scattering operator. $A_\nu(\mathbf{R})$ is thus a smoothly varying field within the crystal and can be represented as a superposition of plane waves.

As in the Laue development we try a substitution of the form

$$A_\mu(\mathbf{R},t)=\sum_\tau A_\mu^\tau e^{i(\mathbf{K}_\tau\cdot\mathbf{R}-\omega_0 t)} \quad \text{(D2)}$$

for the photon field *within* the crystal. Here the $\boldsymbol{\tau}$ are the reciprocal-lattice vectors, $\mathbf{K}_\tau=\mathbf{K}_0+\boldsymbol{\tau}$, and $\mathbf{K}_0\approx\mathbf{k}_0$ is to be determined ($\mathbf{k}_0$ is the wave vector of the incident photon). Substituting (D2) into (D1) and using the integral expression for e^{ik_0x}/x, we have

$$\sum_\tau A_\mu^\tau e^{i(\mathbf{K}_\tau\cdot\mathbf{R}-\omega_0 t)} = A_\mu^0(\mathbf{R},t)+\sum_j\sum_{\tau'}\frac{e^{-i\omega_0 t}}{2\pi^2}\int d^3\mathbf{q}\frac{e^{i\mathbf{q}\cdot\mathbf{R}}e^{i(\mathbf{K}_{\tau'}-\mathbf{q})\cdot\mathbf{R}_j}}{q^2-k_0^2-i\epsilon} \times M_{\mu\nu}(\mathbf{k},\mathbf{K}_{\tau'})A_\nu^{\tau'}. \quad \text{(D3)}$$

To first approximation, we treat $\mathbf{K}_\tau$, as purely real in (D3). [This of course is not correct, but the resulting optical equation (D5) correctly treats absorption to first order.] The sum over R_j, $\sum_j e^{i(\mathbf{K}_{\tau'}-\mathbf{q})\cdot\mathbf{R}_j}$, can then be replaced by $\sum_\tau(2\pi)^3 n\delta^{(3)}(\mathbf{K}_\tau-\mathbf{q})$, where n is the atomic density, and (D3) becomes

$$\sum_\tau A_\mu^\tau e^{i(\mathbf{K}_\tau\cdot\mathbf{R}-\omega_0 t)}=A_\mu^0(\mathbf{R},t)+4\pi n\sum_\tau\sum_{\tau'}\frac{e^{i(\mathbf{K}_\tau\cdot\mathbf{R}-\omega_0 t)}}{K_\tau^2-k_0^2-i\epsilon} \times M_{\mu\nu}(\mathbf{K}_\tau,\mathbf{K}_{\tau'})A_\nu^{\tau'}. \quad \text{(D4)}$$

Applying the D'Alembertain $\Box_{R,t}=\nabla_R^2-\partial_t^2$ to both sides of (D5) and equating the τ components we obtain

$$(\mathbf{K}_\tau^2-k_0^2)A_\mu^\tau=\sum_{\tau'}4\pi n M_{\mu\nu}(\mathbf{K}_\tau,\mathbf{K}_{\tau'})A_\nu^{\tau'}. \quad \text{(D5)}$$

Equation (D5) is the generalization of Laue equation for x-ray optics for the wave field within the crystal. (See, for example, Ref. 3, Eq. 8.23.) For crystals with several atoms per unit cell, and with a complex internal field structure, $M_{\mu\nu}(\mathbf{k},\mathbf{k}')$ is understood to be the scattering operator of the unit cell (chemical, or internal field unit cell, whichever is larger) as given by Eq. (26), and n is the corresponding unit-cell density,

For Mössbauer frequencies we only need to consider the transverse parts of the photon fields, which we denote by $\mathbf{A}^\tau$, $\mathbf{A}^{\tau'}$. Analyzing the fields in terms of orthogonal basis vectors as in Sec. III, we can write (D5) as

$$(\mathbf{K}_\tau^2-k_0^2)\mathbf{A}^\tau=\sum_{\tau'}\tilde{h}^{\tau\tau'}\mathbf{A}^{\tau'}, \quad \text{(D6)}$$

where the matrix $\tilde{h}$ is defined in terms of the matrices $\tilde{f}$ and $\tilde{F}$ of Eqs. (32) and (33) by

$$\tilde{h}^{\tau\tau'}=2k_0\tilde{f}^{\tau\tau'}. \tag{D7}$$

Equation (D6) corresponds to Eqs. (36a) and (40a) and gives the same solutions (to first order).

Off Bragg only the τ_0 channel is open. For a parallel-sided medium, we take $\mathbf{K}_{\tau_0}=\mathbf{k}_0+(f_\eta/\sin\phi_0)\hat{\mathbf{z}}$, and we obtain immediately from Eqs. (D6)–(D7)

$$\tilde{f}^{\tau_0\tau_0}\mathbf{A}^{\tau_0}+f_\eta\mathbf{A}^{\tau_0}. \tag{D8}$$

Equation (D8) is identical to (58), and the subsequent treatment of transmission through a Mössbauer medium carries through unchanged.

For a single-Bragg reflection two channels will be open: the τ_0 channel and a τ_1 channel. For this case, (D6) is explicitly

$$\begin{aligned}(k_0^2-\mathbf{K}_{\tau_0}{}^2+\tilde{h}^{\tau_0\tau_0})\mathbf{A}^{\tau_0}+\tilde{h}^{\tau_0\tau_1}\mathbf{A}^{\tau_1}=0,\\ \tilde{h}^{\tau_1\tau_0}\mathbf{A}^{\tau_0}+(k_0^2-\mathbf{K}_{\tau_1}{}^2+\tilde{h}^{\tau_1\tau_1})\mathbf{A}^{\tau_1}=0,\end{aligned} \tag{D9}$$

where $\mathbf{K}_{\tau_1}=\mathbf{K}_{\tau_0}+\boldsymbol{\tau}_1$, and for a parallel-sided crystal $\mathbf{K}_{\tau_0}=\mathbf{k}_0+\alpha\hat{\mathbf{z}}$. The determinant equation associated with (D9) gives four values of α, and for each value of α we have four amplitudes $A_{\lambda,\alpha}{}^{\tau}$ ($\lambda=x,y$; $\tau=\tau_0,\tau_1$) to be determined. The additional equations necessary to solve for the $A_{\lambda,\alpha}{}^{\tau}$ uniquely are the boundary conditions corresponding to (36b) and (36c) and (40b) and (40c):

$$\sum_{\lambda=x,y}\sum_{\alpha}A_{\lambda,\alpha}{}^{\tau_t}\boldsymbol{\varepsilon}_\lambda{}^{\tau_t}=\boldsymbol{\varepsilon}_0\delta_{\tau_t\tau_0} \tag{D10a}$$

for transmission channels τ_t, and/or

$$\sum_{\alpha}A_{\lambda,\alpha}{}^{\tau_R}e^{i\alpha M}=0 \tag{D10b}$$

for a reflection channel.

Equations (D9) and (D10a) and (D10b) are essentially equivalent to (36) and (40), but are slightly more general in that it has not been necessary to assume that one set of crystalline planes is parallel to the surfaces. If the latter assumption is made, and if, for example, τ_1 corresponds to a reflection channel, then outside the crystal $\mathbf{k}_1=(-g_1,\ \mathbf{k}_{xy}{}^0+\boldsymbol{\tau}_{xy}')$, where g_1 is given by (25a), while inside the crystal $\mathbf{K}_0=\mathbf{k}_0+\alpha\hat{\mathbf{z}}=k'\hat{\mathbf{z}}+\mathbf{k}_{xy}{}^0$ and $K_1=(k'+\tau_z')\hat{\mathbf{z}}+\mathbf{k}_{xy}{}^0+\boldsymbol{\tau}_{xy}'$. We then have $k_0{}^2-K_0{}^2\approx 2g_0(g_0-k')$ and $k_0{}^2-K_1{}^2\approx k_1{}^2-K_1{}^2\approx 2g_1(g_1+\tau_z'+k')$ in (D9). (Note that $g_1+\tau_z'\approx -k'$.) Dividing the two equations of (D9) by $2g_0$ and $2g_1$, respectively, and multiplying through by d, we obtain

$$\begin{aligned}[(g_0-k')d+\tilde{F}^{\tau_0\tau_0}]\mathbf{A}_{k'}{}^{\tau_0}+\tilde{F}^{\tau_0\tau_1}\mathbf{A}_{k'}{}^{\tau_1}=0,\\ \tilde{F}^{\tau_1\tau_0}\mathbf{A}_{k'}{}^{\tau_0}+[(g_1+\tau_z'+k')d+\tilde{F}^{\tau_1\tau_1}]\mathbf{A}_{k'}{}^{\tau_1}=0.\end{aligned} \tag{D11}$$

It is easily verified that (D11) is identical to (36a) to this order.

For the special cases considered in Sec. III for which there is no polarization mixing, there then exists a set of orthogonal basis for which *all* the matrices $\tilde{h}^{\tau'\tau}$ in (D9) are orthogonal. Equation (D8) then separates into two sets of Laue equations, and all the Laue development can be taken over directly (see Refs. 3, 17, and 18).